PFAS Occurrence, Biotransformation, and Transport through Vegetation

Authors and Affiliation:
Dr. Mengyan Li and Dr. Lucia Rodriguez-Freire,
New Jersey Institute of Technology

Prepared for:
New Jersey Department of Environmental Protection
Division of Science and Research

Project Manager: Sandra M. Goodrow, Ph.D.

Date: August 2024

State of New Jersey
Phil Murphy, Governor

Department of Environmental Protection
Shawn M. LaTourette, Commissioner

Division of Science & Research
Nicholas A. Procopio, Ph.D., Director

Visit the DSR website:
https://dep.nj.gov/dsr

Please cite as: Mengyan Li and Lucia Rodriguez-Freire, 2024. PFAS Occurrence, Biotransformation, and Transport through Vegetation. New Jersey Department of Environmental Protection. Trenton, NJ. 54 pages. Available at https://hdl.handle.net/10929/141968

Acknowledgements

This project was partially supported by NJDEP via the award SR21-019 to the New Jersey Institute of Technology (NJIT). We sincerely appreciate the valuable guidance and suggestions provided by Dr. Sandra Goodrow and other colleagues at the Division of Science & Research at NJDEP. The funding of this award was primarily used to help support three graduate students at NJIT, including Chen Wu, Boran Wang, and Boyuan Su, and several undergraduate researchers who work at Dr. Mengyan Li and Dr. Lucia Rodriguez-Freire's labs.

Executive Summary

Contamination of per- and polyfluoroalkyl substances (PFAS) has emerged with increasing concern in New Jersey and other states across the country. In this project, we first developed sensitive and reliable PFAS analytical methods using liquid chromatography coupled with tandem mass spectrometry (LC/MS/MS) and nano-electrospray ionization high-resolution mass spectrometry (Nano-ESI-HRMS). Particularly, analysis by Nano-ESI-HRMS can be complementary to the standard method using LC/MS/MS, since this new approach enables the non-target screening of new PFAS features in environmental and laboratory samples. A standard operating procedure (SOP) for PFAS analysis by this newly developed Nano-ESI-HRMS was generated and attached in the appendix. Second, we further analyzed PFAS in a multimedia environment from four sites in New Jersey. The highest PFAS concentration in surface water was found near the Ringwood Superfund site downstream a waste disposal area on a foamy stream (PFOS 445.56 ng/L). The highest sediment concentration was found near the landfill in Kearny (PFOS replicate range of 3.17-5.79 ng/g). The highest plant concentration was found in Little Pine Lake (PFOS replicate range of 22.79-24.90 ng/g). Perfluorooctane sulfonate (PFOS) was dominantly detected in both plant samples and environmental matrices where the plants were collected, supporting the occurrence of bioaccumulation. Furthermore, perfluorohexanoic acid (PFHxA) was primarily detected in shoot samples of plants, suggesting the uptake and translocation of PFAS from the environment. Using Nano-ESI-HRMS, chloroperfluoropolyether carboxylates (ClPFPECA) in soil and plant samples were screened. However, none of these samples showed significant detection of ClPFPECA, warranting further optimization of the extraction and analytical procedures for the analysis of ClPFPECA in environmental samples. Third, pairing with the observation of PFAS in the field, we characterized the biotransformation of 6:2 fluorotelomer carboxylic acid (6:2 FTCA) by *Rhodococcus jostii* RHA1, a model rhizospheric bacterium. This bacterium exhibited significant biodefluorination activities that can be sustained by the amendment of carbohydrate substrates, such as glucose and fructose. Coupling with the liberation of free fluoride, a 6:2 FTUCA conjugate molecule (m/z = 696.20) was identified as an important biotransformation product of 6:2 FTCA. Such process was regulated by the presence of copper and other metallic anions, though the molecular foundations remains unknown. Collectively, findings of this study underscore the needs to investigate the PFAS contamination and attenuation in the environment and natural biota (i.e., plants and aquatic animals) in the proximity of landfills. This project has contributed to two research publications[1-2] to date.

Contents

List of Tables

List of Figures

Problem Statement/Objectives

Per- and polyfluoroalkyl substances (PFAS) represent a large family of over 7,000 man-made fluorinated organic compounds that are considered as "forever chemicals" with the strong C-F bonds.[3-5] Driven by the widespread occurrence and prominent health risk, New Jersey is a pioneer state in reporting and legislating PFAS contamination. The current drinking water standards for PFOA and PFOS in New Jersey are set at 14 and 13 ng/L, respectively. As one of the most populated states in the US, New Jersey has documented an increasing number of PFAS contamination sites and incidents in the past decade. PFAS contamination was found primarily associated with PFAS manufacture sites and facilities that use or manufacture fluoropolymers.[6] PFAS has also been widely detected at firefighting training areas with historical use of aqueous film forming foams (AFFFs). In addition, New Jersey has a large number of landfill sites (e.g., Ringwood Mines Landfill and Combe Fill North Landfill). These landfill sites are potential point sources that release PFAS and other pollutants to the subsurface.[7]

With the advancement of high-resolution mass spectrometry (HRMS), analysis of PFAS in environmental samples has been extended from target PFAS, primarily perfluorinated sulfonic acids (PFSAs) and perfluorinated carboxylic acids (PFCAs), to non-target PFAS. HRMS enables the identification of molecular formulas that have exact masses within a user-specified mass-error threshold and facilitates informing molecular structures when the molecular-fragment mass spectra are available and adequate.[8] In a recent study, 10 chloroperfluoropolyether carboxylates (ClPFPECA) were identified, with at least three congeners in all samples collected across New Jersey, including soils, surface and groundwater, and vegetation (such as agricultural crops).[6] Lighter congeners also exhibit high mobility and transport remotely to impact downwind areas.[6]

In this project, we aim to develop an approach to analyze ClPFPECA and other non-target PFAS using HRMS in soil, water, and vegetation samples at selected sites in New Jersey. Further laboratory tests will be carried out to investigate the PFAS uptake by plants and biotransformation by rhizospheric bacteria. Specific objectives of this project include:

1. Development of a sensitive approach for the analysis of both target and non-target PFAS using HRMS,
2. Quantification of PFAS concentration in different plants and rhizospheric soils at PFAS-impacted sites in New Jersey,
3. Identification of the environmental factors affecting PFAS uptake and transformation by plants, and
4. Biotransformation of PFAS by bacteria abundant in the rhizosphere.

Task 1. Method Development for PFAS Analysis by HRMS

Background

Method 537.1, Method 533, and Method 1633 are three of the standard methods published by EPA for target PFAS analysis in environmental samples [9-10]. After appropriate sample pretreatment procedures (e.g., solid phase extraction [SPE]), all methods use liquid chromatography coupled with tandem mass spectrometry (LC/MS/MS) for the analysis of an array of target PFAS, such as perfluorinated sulfonic acids (PFSAs), perfluorinated carboxylic acids (PFCAs), and fluorotelomer sulfonic acids (FTSs). LC/MS/MS-based PFAS analysis can be relatively time- and labor-consuming. First, these methods involve many operational parameters (e.g., the ingredient and gradient of mobile phases) that demand adaptation and optimization to achieve satisfactory separation and sensitivity of individual target PFASs, and such process can become challenging with the increasing number of target analytes [11-12]. Further, LC separation typically takes 10~30 min for each run [12-16]. Considering the large sampling size for field investigation, it is of significant value to develop PFAS analytical approaches that can be easily adapted and allow rapid analysis. Furthermore, LC/MS/MS is not best suited for non-target PFAS analysis due to the limitation of mass resolution below 10,000[1] that won't provide mass accurate enough for addressing the molecular formula and structure [17].

In this project, we combined nano-electrospray ionization (Nano-ESI) with HRMS for both target and non-target PFAS analysis. Nano-ESI refers to ESI that is equipped with an ultrathin emitter (usually 10~100 micrometer in diameter) that can be electrified at high voltage (~kV) to produce nanodroplets, promoting efficient ionization and diminishing salt interference as compared to conventional ESI[11, 18-19]. Therefore, even with a small injection volume (e.g.,1 μL), Nano-ESI can generate a signal intensity 2 to 3 times higher than that detected by conventional ESI.[20] Furthermore, the emitter can be easily replaced for each sample to avoid cross-contamination from prior injections[11, 19]. As there is no chromatographic separation, the running time for Nano-ESI can be as short as 1.5 min. Collectively, Nano-ESI is an advantageous injection method that promotes sensitive and rapid PFAS analysis with minimal sample volume requirement.

Given the increasing number of newly identified PFASs, interest in screening and quantitative analysis of these non-target PFASs by high-resolution mass spectrometry (HRMS) has escalated over the past decade [21-27]. HRMS enables accurate screening (i.e., mass error $\leqslant$5 ppm) of mass features due to its high spectral resolving power (e.g., 140,000 for Orbitrap) without a prior need for standards that are either expensive or inaccessible [22, 28-29]. Collision-induced dissociation (CID) can be further employed for identifying the fragmentation pattern and determining the relative position of moieties within a molecule of interest [30], allowing structural prediction and validation [31-33].

Here we established the PFAS analysis by both Nano-ESI-HRMS and LC/MS/MS and compared their detection sensitivity and accuracy of 22 target PFAS (Table 1), including PFCAs, PFSAs, fluorotelomer carboxylic acids (FTCAs), FTSs, and HFPO-DA. Furthermore, Nano-ESI-

[1] This is dimensionless as the formula is (m1-m2)/m2

HRMS enabled PFAS suspect screening to identify a biotransformation metabolite produced over activated sludge treatment. A standard operating procedure for PFAS analysis by this newly developed Nano-ESI-HRMS is generated and attached in the appendix. The development of this novel analytical approach with Nano-ESI-HRMS has prominent potential to assist and promote the imminent investigation of fate, behavior, and exposure of PFASs in water and other matrices.

Table 1 Structure and quantification information of 22 target PFAS

Analyte	structure	group	internal standard (IS)
PFBS	$F(CF_2)_nSO_3H$	PFSA	M8-PFOS
PFHxS			
PFHpS			
PFOS			
PFDS			
PFBA	$F(CF_2)_nCOOH$	PFCA	M8-PFOA
PFPeA			
PFHxA			
PFHpA			
PFOA			
PFNA			
PFDA			
PFUdA			
PFDoA			
PFTrDA			
PFTeDA			
5:3 FTCA	$F(CF_2)_n(CH_2)_mCOOH$	FTCA	M2-6:2 FTCA
6:2 FTUCA			
6:2 FTCA			
6:2 FTS	$F(CF_2)_nCH_2CH_2SO_3H$	FTS	M2-6:2 FTS
8:2 FTS			
GenX	C_3F_7-O-CF(CF_3)-COOH	HFPO-DA	M8-PFOA

Project Design and Methods Quality Assurance

Chemicals and Reagents. The PFCA mixture standard (C4-C14), PFSA mixture standard (C4, C6, C7, C8, and C10), 6:2 FTUCA standard, 5:3 FTCA standard, 6:2 FTS standard, and mass-labeled PFAS standards (M8-PFOA, M8-PFOS, M4-PFHxS, M2-6:2 FTCA, and M2-6:2 FTS) were all purchased from Wellington Laboratories Inc. (Guelph, Ontario, Canada) with the purity of >98%. 6:2 FTCA (3,3,4,4,5,5,6,6,7,7,8,8,8-tridecafluorooctanoic acid, >97%) and 5:3 FTCA (2H,2H,3H,3H-perfluorooctanoic acid, >97%) were purchased from Synquest Laboratories (Alachua, FL, USA). Reagent grade trifluoromethanesulfonic acid (TFMS) was purchased from Sigma-Aldrich (St. Louis, MO, USA). LCMS grade ammonia acetate (>99%) was purchased from

Sigma-Aldrich (St. Louis, MO, USA). LCMS grade methanol (>99%) was purchased from Fisher Chemicals (Hampton, NH, USA). Ultrapure water obtained from the Milli-Q RC Synthesis water purification system (Millipore, Bedford, MA, USA) was used in the experiments.

As suggested by EPA method 537.1, a mixed internal standard (IS) solution consisting of 4 mass-labeled PFASs (M8-PFOA, M8-PFOS, M2-6:2 FTCA, and M2-6:2 FTS in Table 1) was prepared at the concentration of 500 μg/L, targeting the quantification for the four main groups of PFASs (i.e., PFCAs, PFSAs, FTCAs, and FTSs). This mixed IS solution was added to calibration solutions and samples to achieve a concentration of 10 μg/L prior to the analysis by Nano-ESI-HRMS or LC/MS/MS. M4-perfluorohexanesulfonic acid (M4-PFHxS) was used as a surrogate to track the efficiency of PFAS extraction in wastewater samples [34-35]. The surrogate stock solution was prepared by diluting its commercial standard solution with methanol (with 4% DI water) to achieve the concentration of 200 μg/L for M4-PFHxS [36].

Laboratory fortified blanks (LFBs) were prepared with 250 mL of reagent water, to which 5 μg/L of the method analytes (i.e., 22 target PFASs listed in Table 1), and all the preservation compounds were added. Laboratory reagent blanks (LRBs) were prepared with 250 mL reagent water in HDPE bottles in the laboratory. LRBs and LRBs were preserved, stored, and processed at the same conditions as all field samples.

Target PFAS Analysis by Nano-ESI-HRMS. PFAS analysis by Nano-ESI-HRMS was operated by a high-resolution Q Exactive hybrid quadrupole−Orbitrap mass spectrometer (Thermo Fisher Scientific, San Jose, CA) equipped with a Nano-ESI injector (Figure 1). The emitter tip was pulled using a laser puller (Model P-2000, Sutter Internet, Novato, CA). The capillary temperature was set at 350 °C. The sample injection flow rate was 2 μL/min with -3.0 kV potential applied to the Nano-ESI emitter. The resolution of 140,000 was selected for the HRMS with the spectra obtained based on a scan time of 2.0 min (80 scans). MS spectra results were not collected until the automatic gain control (AGC) target achieved 100% with the total ion current (TIC) variation below 10%. MS1 data were collected under the full scan mode in the range of 50~750 m/z with no collision energy applied. Based on the suspect screening result of MS1 data, potential m/z species were manually selected for CID to collect MS2 data. For select mass species of interest, MS2 data were collected under the data-dependent acquisition (DDA) mode when CID was manually applied. The quadrupole filter was set to distinguish the mass difference of ±0.2 Da at m/z 200, resulting in a full width half maximum (FWHM) resolution of 500 (=m/dm). When two or more molecules were captured by MS1, parent ions and their daughter ions were determined

based on their co-occurrence in the MS2 spectrum and the intensity shifting pattern in response to the applied collision energy (CE).

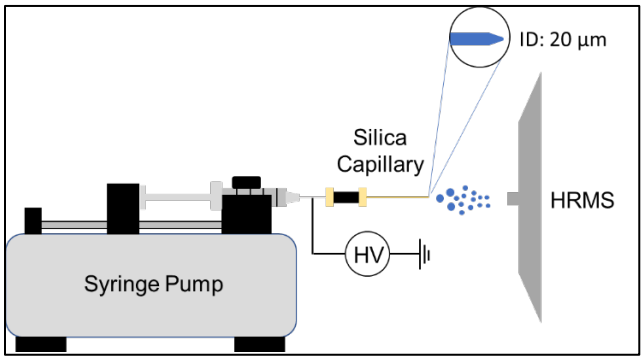

Figure 1 Schematic of Nano-ESI-HRMS (with nanodroplets)

Target PFAS Analysis by LC/MS/MS. For LC/MS/MS analysis, following the EPA Method 537.1 and previous studies [11-12], 22 target PFASs were analyzed using a 1290 Infinity II HPLC system in tandem with 6470A triple quadrupole mass spectrometer (Agilent, Santa Clara, CA)[37]. Aliquots (10 µL) were injected into this LC/MS/MS system equipped with a Symmetry C18 column (ID 2.1 mm, length 100 mm, particle size 3.5 µm) (Waters, Milford, MI) at a flow rate of 0.3 mL/min. The mobile phase initially consisted of 80% solvent A (5 mM ammonia acetate in 10% (v/v) methanol), decreased to 40% A with 60% solvent B (pure methanol) in 2.0 min, further reduced to 20% A in 1 min and kept for 5 min, and then changed back to 80% A in 1 min and held for 4.5 min. Triple quadrupoles mass spectrometer was set in the negative-ion electrospray mode. Multiple reaction mode (MRM) was set for ion collection. The pressure in the nebulizer was set at 25 psi with a capillary voltage of -3.5 kV. The desolvation gas temperature was 350 °C, with a flow rate of 8 L/min. MS data were processed using the MassHunter QQQ quantitative analysis software (Agilent Technologies, USA).

Laboratory Calibration and Lower Limits of Detection (LODs). A primary dilution standard (PDS) solution was prepared for the calibration of 22 target analytes (Table 1) via the dilution of the stock standard solutions in methanol (with 4% DI water) to achieve a concentration of 200 µg/L for each analyte. This PDS solution was serially diluted to prepare ten-point calibration solutions with 39 to 20,000 ng/L concentrations. All calibration solutions were prepared in triplicates, and their average mass intensities were used for constructing the calibration curves when the regression linearity met $R^2 > 0.99$. To assess the analytical sensitivity, the lower limits of detection (LODs) were determined for 22 target PFASs using the formula $3*S_B/m$, where S_B is the standard deviation of the target observed in blank controls and m is the slope of the calibration curve[38-39]. In case that a LOD is above the lowest calibration concentration (i.e., 39 ng/L), it is recalculated with the corrected slope after removing the lowest calibration point until the new LOD is below the lowest concentration used in the calibration.

Non-target PFAS Screening. Following Barzen-Hanson's work [27], the suspect screening method was developed to process Nano-ESI-HRMS data, consisting of four steps: local database construction, background noise removal, positive hit screening, and molecular structure validation.

Non-target screening and analysis were processed on a local computer equipped with an Intel i9-9900KF (8 cores, 16 threads) processor, an 8 GB RTX 2070 graphic card, and a group of 64 GB memory in Li's lab. A local PFAS database, consisting of the chemical formulae, SMILES structures, monoisotopic molecular weights, and putative monoisotopic anionic weight of ~7,300 PFASs, was constructed based on the Master List of PFAS Substances[40] and timely updates from recent publications[8, 13, 21, 27, 41-50]. For each sample, the Nano-ESI-HRMS analysis generated a list of mass species (*m/z*) and their intensities as MS1 data exported by Xcalibur (ThermoFisher Scientific, USA) from the raw HRMS data file. Background mass species were subtracted from the samples' peak list by traversal comparison between laboratory reagent blanks (LRBs), methanol solvent controls, and samples, according to the following criteria: (1) the mass ion occurred in > 50 scans per sample, (2) the mass ion was positively detected in all replicates, and (3) its average relative intensity (RI, the ratio of target ion intensity to that of the internal standard M8-PFOS) in samples was at least 100 times higher than in that in solvent/reagent blanks (if existed). Only the ion species with RI of >0.1% were further processed for structure validation and semi-quantified PFAS profiling.

After removing background noises, mass spectra were matched with those in our local database based on a mass error threshold of 5 ppm. All positive hits were gathered as a suspect screening list and ranked by intensity with a cutoff at 10^5 (a.u.). Ions' structures were further examined based on the fragmentation patterns in MS2 data obtained by CID. Positive mass values were used to solve their possible molecular formulas according to the monoisotopic mass of elements (i.e., C, F, H, and O). The unsaturation degree was set between 0 and 5 for initial screening. All the possible formulas for positively screened mass were used to match with online chemical database (e.g., Chemspider, Pub Chem, KEGG, and NORMAN) for the prediction of their molecular structures. The confidence levels of suspect PFASs were then determined following the rules indicated by Schymanski et al.[51]

Results and Discussion

Sensitive and Accurate PFAS Analysis by Nano-ESI-HRMS. For 22 target PFAS analyte, ten-point calibration curves with DI water spiked with individual PFAS in the concentration range between 39 to 20,000 ng/L. All calibration curves were prepared in triplicates. Using their average mass intensities, the regression linearity met $R^2 > 0.99$ for the calibration curves of all 22 target analytes as shown in Figures 2 through 4.

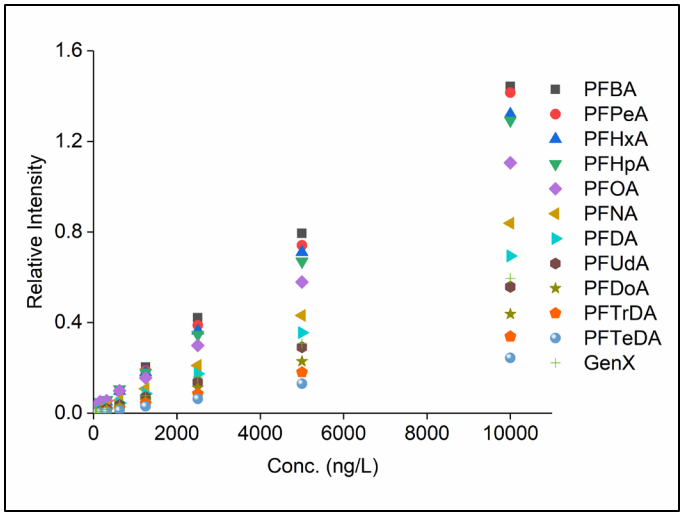

Figure 2 Data points to construct calibration curves for 11 PFCAs and GenX by Nano-ESI-HRMS

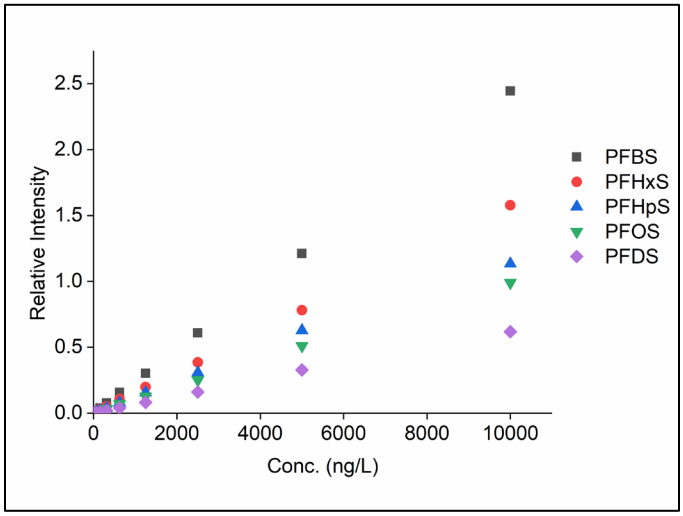

Figure 3 Data points to construct calibration curves for 5 PFSAs by Nano-ESI-HRMS

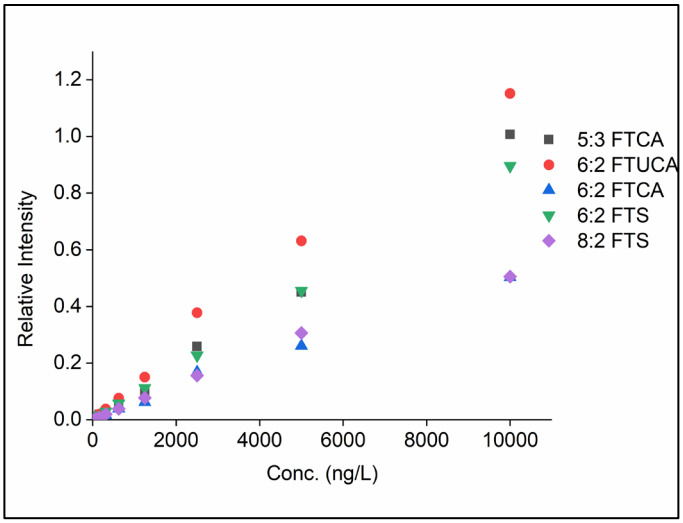

Figure 4: Data points to construct calibration curves for 3 FT(U)CAs and 2 FTSs by Nano-ESI-HRMS

Detection by Nano-ESI-HRMS also exhibited high sensitivity for the analysis of 22 target PFASs, achieving low LODs in the range from 3.2 to 36.2 ng/L (Table 2). For LC/MS/MS, good separation was achieved of all 22 target analytes, though their LODs exhibited a two-order-of-magnitude span from 1.1 to 135.6 ng/L (Table 2). Our LC/MS/MS method was optimized for detecting C4-C8 PFSAs and C6-C8 PFCAs that are of primary concern by regulatory agencies with LODs in the range of 1.1 to 15.2 ng/L. However, this method was less sensitive in detecting precursor compounds, particularly FTSs and GenX, with LODs greater than 60 ng/L. In contrast, Nano-ESI-HRMS exhibited sensitive detection of both C4-C8 perfluoroalkyl acids (PFAAs) and precursor compounds (e.g., FTCAs, fluorotelomer unsaturated carboxylic acids [FTUCAs], FTSs, and HFPO-DA). For these precursor compounds, LODs of Nano-ESI-HRMS were 1.2 to 15.6 folds lower than those of LC/MS/MS. Compared to LC/MS/MS, Nano-ESI-HRMS showed similar or higher sensitivity towards all target PFASs of different chain lengths and functional moieties, likely due to the uniformly formed nanodroplets (shown in Figure 1) precluding bias derived from the chromatographic separation and solvent elution.

Table 2: Instrument LODs and R2 of Calibration Curves for 22 Target PFAS Analytes by Nano-ESI-HRMS and LC/MS/MS

Category	Analyte	Nano-ESI-HRMS		LC/MS/MS	
		LOD (ng/L)	R^2	LOD (ng/L)	R^2
PFSAs	PFBS	20.4	0.9997	2.3	0.9970
	PFHxS	25.1	0.9999	1.3	1.0000
	PFHpS	6.6	0.9996	1.1	0.9983
	PFOS	14.0	0.9999	4.0	0.9999
	PFDS	4.2	0.9999	4.6	0.9997

PFCAs	PFBA	24.3	0.9998	58.5	0.9996
	PFPeA	14.5	0.9997	15.2	0.9995
	PFHxA	14.2	0.9999	8.0	0.9999
	PFHpA	26.4	1.0000	13.9	0.9968
	PFOA	36.2	0.9999	9.5	0.9981
	PFNA	3.3	0.9999	14.2	0.9905
	PFDA	4.3	0.9996	87.8	0.9987
	PFUdA	6.8	0.9998	51.8	0.9997
	PFDoA	10.7	0.9991	31.7	0.9999
	PFTrDA	7.0	0.9998	42.7	0.9996
	PFTeDA	9.3	0.9999	50.2	0.9999
FT(U)CAs	5:3 FTCA	22.7	0.9996	28.1	0.9937
	6:2 FTUCA	12.4	0.9999	20.1	0.9972
	6:2 FTCA	3.2	0.9998	6.7	0.9991
FTSs	6:2 FTS	7.5	1.0000	66.3	0.9991
	8:2 FTS	8.7	0.9999	135.6	0.9996
HFPO-DA	GenX	6.4	0.9999	96.6	0.9997

The precision (% RSD) and accuracy (% recovery) for the Nano-ESI-HRMS analysis were further assessed by a surrogate-corrected recovery experiment with 7 LFB replicates spiked with 5 ng of 22 target PFASs. As shown in Figure 5a, the precision (2~11%) reflected the high repeatability and reliability of PFAS analysis by Nano-ESI-HRMS. Figure 5b showed mean surrogate-corrected recovery rates between 87% and 120% for 16 PFASs. Five PFASs (i.e., perfluorododecanoic acid [PFDoA], PFHxS, 5:3 FTCA, 8:2 FTS, and HFPO-DA) had recoveries between 120% and 130%, and perfluoroundecanoic acid (PFUdA) had a mean recovery of 133%. The recoveries in the range of 87~133% met the requirement of EPA Method 537.1 (50~150%). They presented a comparable performance to previous records for the analyses of PFCAs, PFSAs, and FTSs (87~99% [48], 70~149% [11], and 80~134% [12]), validating the effectiveness and robustness of Nano-ESI-HRMS for the analysis of mixed PFASs at environment-relevant concentrations.

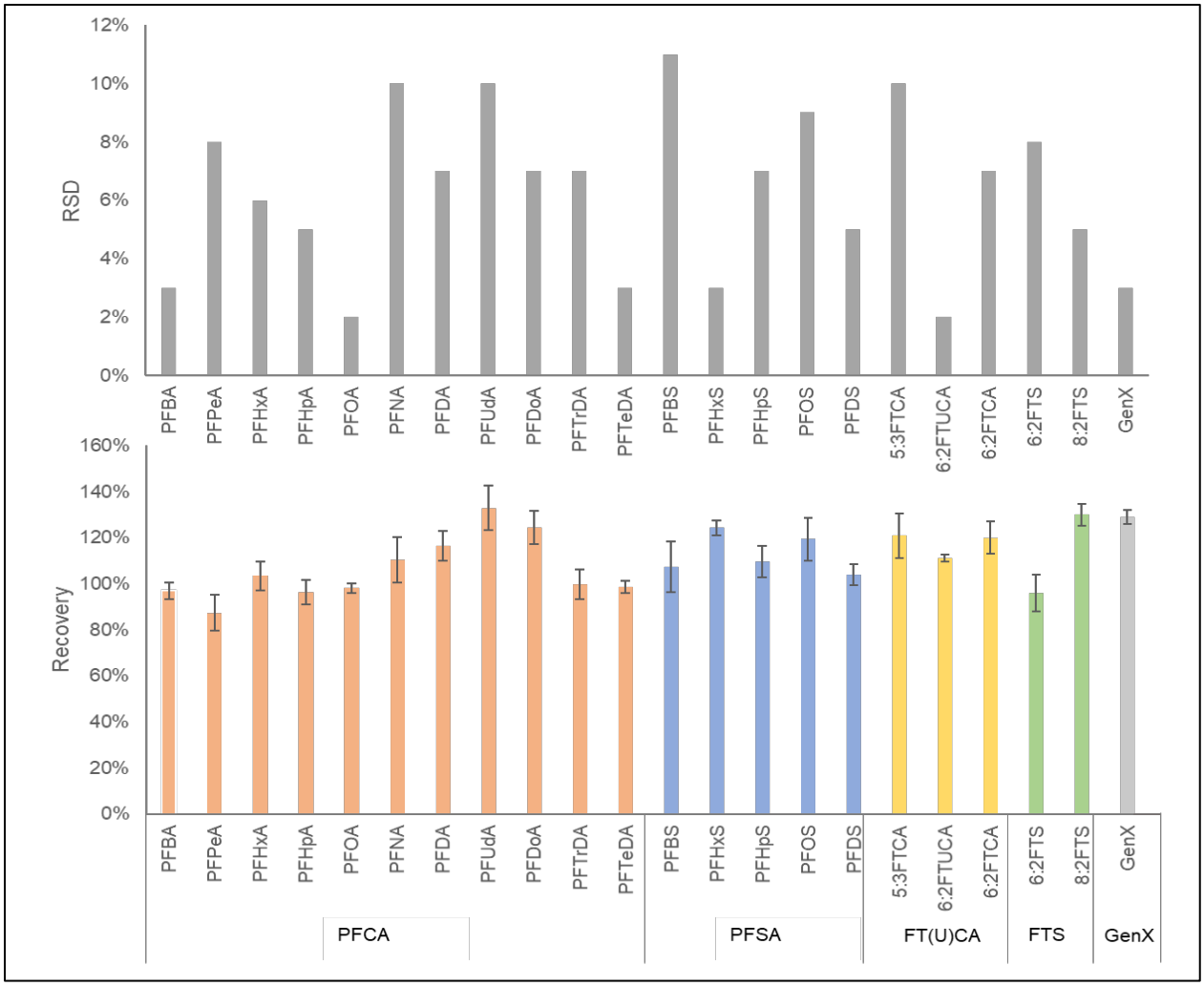

Figure 5 Precision (a) and accuracy (b) of the Nano-ESI analysis for the 22 target PFASs as determined by the surrogate-corrected recovery experiment of 7 LFB replicates (error bar shows ± 1 standard deviation). PFASs are grouped into 5 classes, including PFCAs (orange), PFSAs (blue), FT(U)CAs (yellow)

Non-target PFAS analysis by Nano-ESI-HRMS. Suspect screening by Nano-ESI-HRMS was conducted to screen for metabolites generated from 5:3 FTCA biotransformation by activated sludges collected from New Jersey wastewater treatment plants [1]. Coupling with 5:3 FTCA biotransformation, a less-fluorinated 5:3 FTUCA intermediate (IUPAC name: 4,5,5,6,6,7,7,8,8,8-decafluorooct-3-enoic acid) was first detected as an important metabolite. This intermediate was detected on day 3 and day 5 and fully vanished on day 7 in all treatments, though with the low detection at relative intensities (RIs) in the range between 0.012 to 0.069 (equivalent to <0.5 μM when estimated using the calibration of 5:3 FTCA). Compared to 5:3 FTCA, this intermediate has one less fluorine and hydrogen, forming a double bond between the fluorinated β and non-fluorinated γ carbons possibly via dehydrogenation (Figure 6).

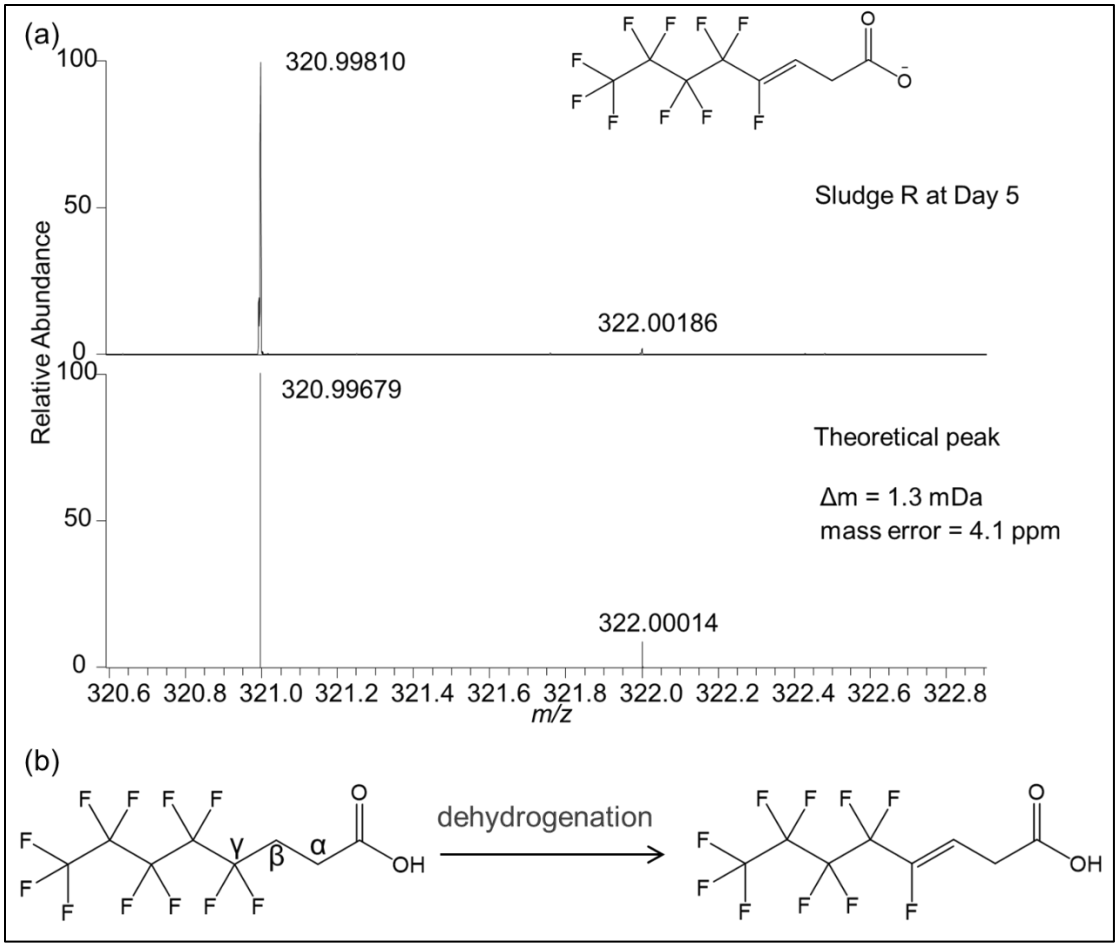

Figure 6 Detection of a 5:3 FTUCA metabolite (4,5,5,6,6,7,7,8,8,8-decafluorooct-3-enoic acid) in 5:3 FTCA treatments inoculated with Sludge R for 5 days as compared to its theoretical spectrum (a) indicating the biodefluorination of 5:3 FTCA at the γ carbon (b).

Task 2: PFAS Contamination Survey in Soils and Plants

Background

New Jersey has set the maximum contaminant levels for PFNA (13 ng/L), PFOS (13 ng/L), and PFOA (14 ng/L) in drinking water to be protective of human health. Determining the source to the environment and the cycling of the PFAS in the environment is of great significance. The following five sites are possibly contaminated with PFAS because of historical or current operations. The Ringwood site (near the Ford Superfund Site) is in north New Jersey next to New York state, which was a historical mining district and paint sludge disposal area for Ford Motor Company in 1970s. The site is known for lead, arsenic, chloroethane, benzene, and 1,4-dioxane as the main contaminants of concern. Battlefield Park is near the Solvay Specialty Polymer site in

south New Jersey. The Solvay industrial site produces high-performance thermoplastic resins and fluoroelastomers and fluorinated gases and liquids. This chemical company stated that they stopped using PFNA in 2010. The next location near Little Pine Lake was selected based on results from a previous PFAS study conducted by the NJDEP Division of Science and Research due to the impoundment receiving drainage from the western edge of the Joint Base McGuire-Dix-Lakehurst (JB MDL). In previous studies by NJDEP, this location had the highest total PFAS level of surface water among 11 waterways in the previous studies, highest total PFAS concentration (30.93 ng/g, PFOS in majority) of sediment samples of 10 sites, and highest total PFAS level in fish samples[52-53]. The New Jersey Meadowlands Commission (NJMC1-E) landfill is approximately 409 acres in size along the western border of the New Jersey Meadowlands between Hudson County and Bergen County. It is currently used as a combination of leaf compost facility and transfer station. Keegan Landfill is approximately 110-acre in size and was operated as a landfill between the 1940's and 1972. This site is next to the 1-E landfill and bordered on the southeast and east by wetland areas and open water wetland, which are potentially impacted by PFAS[54].

The concentration and distribution of PFAS in water, soils, and plants were investigated at suspected PFAS-impacted sites in New Jersey.[55] Following the published results by Goodrow, samples were also collected along the Passaic River, and at an additional location near Little Pine Lake near the JB MDL. In addition to the samples collected at Woodbury Creek at Battlefield Park near the Solvay Specialty Polymers manufacturing facility in West Deptford, samples were collected in the wetlands near the Keegan and NJMC-1 landfills in Kearny. Between 3 – 5 plants were collected per location, with their soil, rhizosphere, and water. The concentration of PFAS and other trace elements, in particular iron, zinc and manganese, in water, soils, and plants were measured at various locations and times of the year. Water and sediment samples were also collected from the Passaic River at the Kearny Riverbank. In all, environmental media samples were collected from six sites (Ringwood, Battlefield Park, Pine Lake 1- Lake, Pine Lake 2- Bridge, NJMC-1-E Landfill, and the Passaic River) as shown in Table 3.

Table 3: Description of sampling locations and type of samples collected

Sampling location	Coordinates	Description of the site	Number of samples	Type of samples	Sampling date	Type of Analysis
Ringwood	41° 8' 12.73"N, 74° 16' 13.12"W	Samples collected downstream OCDA and PMP, and at the PMP/CN intersection, near Ford Superfund site	3 water samples 5 sediment samples 5 plants	Water, sediments, plants	Jun-20	QQQ PFNA, PFOA, PFOS
Battlefield Park, West Deptford, New Jersey	39°51'55.5"N 75°11'40.6"W	Next to Solvay Specialty Polymers, across the Woodbury Creek	3 water samples 5 soil/sediment samples 5 plants	Water, sediments, plants	Sep-21	QQQ PFBS, PFHpA, PFHxA, PFHxS, PFNA, PFOA, PFOS
Little Pine Lake 1- Lake, Pemberton Township, New Jersey	39°59'25.7"N 74°34'14.3"W	Downstream Joint Base McGuire-Dix-Lakehurst, in the Bayberry Park area	2 water samples 2 soil samples 3 plants	Water, sediments, plants	Oct-21	QQQ PFBS, PFHpA, PFHxA, PFHxS, PFNA, PFOA, PFOS
Little Pine Lake 2- Bridge, Pemberton Township, New Jersey	39°59'32.1"N 74°34'10.6"W	Downstream Joint Base McGuire-Dix-Lakehurst, next to Range Rd bridge, downstream Jack run	6 water samples 2 soil samples 3 plants	Water, sediments, plants	Oct-21	QQQ PFBS, PFHpA, PFHxA, PFHxS, PFNA, PFOA, PFOS
NJMC-1 landfill, Kearney, New Jersey	40°46'02.5"N 74°07'22.8"W	Under a bridge, next to a stream flowing parallel to the landfill. There was a leachate outlet coming from the landfill	2 water samples 3 plants	Water, sediments, plants	Apr-22	QQQ PFBS, PFHpA, PFHxA, PFHxS, PFNA, PFOA, PFOS

Sampling location	Coordinates	Description of the site	Number of samples	Type of samples	Sampling date	Type of Analysis
Passaic River, Kearney Riverbank Park, Kearney, New Jersey	40°45'50.2"N 74°09'31.4"W	In front of the Riverside Superfund Site, at a boat launching area	2 water samples 3 soil samples	Water, sediments,	October 2021 – no plants collected	QQQ PFBS, PFHpA, PFHxA, PFHxS, PFNA, PFOA, PFOS

Project Design and Methods Quality Assurance

Sample Collection. The samplings were carried out in spring and fall seasons, considering low temperatures during wintertime result in poor plant growth. Photosynthesis is slow at low temperatures. Since photosynthesis is slowed, growth is limited, and this results in low PFAS uptake and accumulation. In Spring and Summer, plant growth boosts and accumulation can increase. In addition, the river flow are not enough for sampling in summer due to the high temperature caused evaporation. The Ringwood site sampling campaign was carried out in May 2019, sampled at one downstream a paint sludge disposal area outside the superfund site and less than 3 km from a school, foam was observed on the stream, the plants were collected on the bank of the little steam; The Battlefield Park sampling campaign was carried in September 2021, water sample was collected from the Delaware river on the north side around 2 km to the Solvay Specialty Polymer site, plant samples were collected on the bank of the river. The Little Pine Lake sampling campaign was carried out in October 2021, one location was the lake, and the other location was a wetland area under the Range Road bridge crossing on the north branch of the lake. The sampling location for the landfill is outside the NJMC1-E landfill and 1.6 km to the Keegan Landfill and the sampling was carried out in April 2022. One drain creek and one small creek near outside the landfill was the two locations selected for sampling. Pictures of select sampling sites can be seen below. Pictures taken on the sample collection days at Ringwood, and NJMC1-E Landfill can be seen in Figure 7, below.

Figure 7: (A) Location in Ringwood when the samples were collected (B) Drain creek outside the NJMC1-E Landfill (C) Small creek near the NJMC1-E Landfill.

The water samples were collected and filled full of 250 mL polypropylene bottles; the pH of the water was recorded at the sampling site using a portable pH meter (Orion Star A329, Thermo Scientific, USA). Sediment and soil samples were collected with Ziplock bag, plant samples were fully collected with paper bags. Water and sediment samples were transported in cooler with ice and stored in refrigerator to keep the temperature around 4 ℃. All containers and sampling tools used during the process were carefully operated to avoid the introduction of contamination.

Chemicals and Standards. A total of 7 PFASs were analyzed, including perfluorohexanoic acid (PFHxA), perfluoroheptanoic acid (PFHpA), perfluorooctanoic acid (PFOA), Perfluorononanoic acid (PFNA), perfluorobutane sulfonic acid (PFBS), perfluorohexane sulfonic acid (L-PFHxS), perfluorooctane sulfonic acid (PFOS), the standards were purchased from Wellington laboratories (Ontario, Canada). The LCMS grade methanol purchased from Sigma-Aldrich (USA). High purity water (18 MΩ cm-1) produced with a Milli-Q system (GenPure Pro standard, Thermo scientific). 6-mL solid phase extraction (SPE) cartridge was purchased from Agilent (Cat. No. 1225-5021, USA). Nitrogen gas (industrial grade, >99% purity) was purchased from Airgas (USA).

PFAS Extraction from Liquid and Solid Samples. The PFAS in water samples was extracted followed EPA method 537.1[56]. After water samples were equilibrated at room temperature, the whole bottle (250 mL) of water samples was passed through a cleaned and conditioned cartridge, then eluted with 8 mL methanol. The cartridges were cleaned by passing through 15 mL methanol and conditioned by passing through 18 mL Milli-Q water. The eluted methanol was collected in clean polypropylene (PP) centrifuge tubes, then concentrated under a gentle stream of nitrogen to 1 mL. The total volume of passed through water sample was measured by weighting the sample bottles before and after extraction.

Sediment and soil samples were dried in oven with 57 ± 2 ℃. Plant samples were raised with ultra-pure Milli-Q water then dried under room temperature. Plant samples were separated to root, stem, and leaf (if appliable, some plants only have shoot), and then homogenized. One gram of dried soil sample or 0.5 gram of plant sample was transferred to a 15 mL polypropylene centrifuge tube containing 6 mL MeOH. Followed with vortexing for 60 seconds, shacked on an

orbital shaker (ELMI™ 20 mm Amplitude, Fisher scientific, Pittsburgh, PA, USA) at 300 rpm for 20 minutes, ultra-sonicated for 30 minutes, then centrifugation at 2,500 rpm for 15 minutes (Sorvall™ ST 8R, Thermo scientific, USA). The aqueous supernatant was collected in another 15 mL clean polypropylene centrifuge tube, then the extraction process was repeated. All collected supernatant volumes were combined and concentrated under a gentle stream of nitrogen to 1 mL.

Quantification of PFAS Using LC-MS/MS. The determination in extracts were using high performance liquid chromatography coupled to triple-quadrupole (QQQ) mass spectrometry (Agilent 1290 Infinity II coupled to Agilent 6470 Triple Quadrupole mass spectrometer). All extracts were filtered by 0.2μm syringe filter for LC-MS/MS analyze. The analytes were separated by Agilent ZORBAX Eclipse Plus C-18 (3.0×50 mm 1.8 μm) HPLC column maintained at 40℃ and eluted with mobile phase A (5 mM Ammonium Acetate in water) and mobile phase B (5 mM Ammonium Acetate in 95% MeOH and 5% water) at a flow rate of 0.5 mL/min. The separation gradient method starts at holding 20% B from 0-0.5 min, 0.6-7 min 95%B, and hold 20%B for another 2 min to stabilize column. The sample injection volume was 5 μL. The parameters of triple quadrupole mass spectrometer were set as follow: gas temperature 230 ℃, gas flow 4 L/min, nebulizer 225 psi, sheath gas temperature 350 ℃, sheath gas flow 12 L/min, capillary positive 3000 V negative 2500 V, nozzle voltage positive 500 V and negative 0 V.

Calculation of bioconcentration and translocation factors. The bioconcentration factor (BF) can be used to evaluate the content of PFAS of plant uptake, which is defined as the ratio of the PFAS concentration in root (ng/g dry weight) over the concentration of PFOA in rhizosphere soil (ng/g dry weight, Eq 1), and the translocation factor (TF) can be used to measure the amount of PFAS transferred from one organ to another, which is defined as the ratio of the PFAS concentration in shoot over the concentration in root (Eq 2)[57-58]. Thus, BF reflects PFAS plant uptake from the environment, while TF reveals the transport of PFAS within the plant, from root to shoot.

$$Bioaccumulation\ factor\ (BF) = \frac{PFAS\ concentration\ plant\ root\ (ng/g)}{PFAS\ concentration\ in\ soil\ (ng/g)} \quad (1)$$

$$Translocation\ factor\ (TF) = \frac{PFAS\ concentration\ in\ shoot}{PFAS\ concentration\ in\ root} \quad (2)$$

Soil organic carbon analysis. The soil organic carbon (SOC) was determined by a commercial laboratory (Agvise Laboratories, Northwood, ND) using the dry combustion method, generally the SOC was calculated by measuring total carbon (TC) and inorganic carbon IC using the TOC instrument (SSM-5000A, SHIMADZU, Kyoto Japan), the measurement of TC was carried by combustion 100 mg soil under 900℃, and the IC was measured by adding 0.5ml 85% phosphoric acid (H_3PO_4) to 100 mg soil sample then combustion under 200℃, the CO_2 from both processes were measured for the calculation. The soil-water partition coefficient, K_D, is calculated

as equation 3:

$$K_{DLan} = \frac{[PFAS]_{Soil,equilibrium}}{[PFAS]_{water,equilibrium}} \quad (3)$$

DNA extraction from soil and root microbial communities. The microbial communities were characterized using Illumina Sequencing from DNA extracts. Microbial community DNA samples were extracted from the soil, rhizosphere (outside) and endosphere (inside) of the plant roots. Phosphate buffer saline (PBS, 8g /L NaCl, 0.2 g/L KCL, 1.15 g/L Na_2HPO_4, 0.2 g/L 0.203 g/L $NaH_2PO_4 \cdot H_2O$, pH=7.3) and saline buffer (SB, 6.0 g/L $NaH_2PO_4 \cdot H_2O$, 150 mM NaCl, pH 7.6) were prepared and sterilized for the rhizosphere and endosphere of the root DNA extraction, respectively. The root fragments were mixed with PBS following a ratio of 0.3 g/10 mL and vortexed for 5 min. The aqueous mixture was used for the DNA extraction of the rhizosphere microbial community. For the DNA extraction of the endospheric microbial community, the root surface was disinfected with 2% sodium hypochlorite solution followed by wash with sterile high purity water, then socked in 70% ethanol for 1 min and rinse with sterile high purity water. The root fragments were cut into small pieces and socked in 10 mL SB and incubation at 200 rpm in 4 ℃ for 4 hours. The solutions from the rhizosphere and endophytic microbial community were then processed using the DNA extraction kit (FastDNA TM, MP Biomedicals, OH, USA). The extract DNA samples were frozen and sent to Molecular Research DNA LP for MiSeq Illumina Sequencing. The data was then processed for statistical analysis at the OTU based level (*Mothur*[2]*)* for alpha-diversity and microbial communities of different samples were compared using NMDS.

Results and Discussion

The extent and distribution of PFAS in different locations of New Jersey was investigated. PFOA, PFNA and PFOS were the only three PFAS analyzed at this site. PFHxA, PFHpA, PFOA, PFNA, PFBS, PFHxS and PFOS were analyzed, except that PFOA, PFNA and PFOS were only analyzed at the Ringwood/Ford Superfund site. All seven PFAS were detected in all the water samples for these four locations, however, PFOS was the only contaminant detected in all the sediment samples. The type of plants was identified by dropping pictures to *Plant identify* online. Information on the samples collected and the description of the locations are provided in Table 3.

In the Ringwood location, the PFOS in water samples (pH=7.28) was measured as high as 445.56 ng/L, PFOA 23.78 ng/L and PFNA 25.69 ng/L in water sample collected where foam was observed. PFNA was not detected in the sediment or plant samples. The average and standard

[2] *Mothur* is an open-source software package for bioinformatics data processing (Accessed here: https://mothur.org/ on 10/17/2024.)

deviation PFOA concentrations in sediment and rhizosphere soil samples are 0.44 ± 0.01 ng/g and 0.5 ± 0.23 ng/g, and 3.23 ± 0.16 ng/g in plant samples. The PFOS concentrations in sediment and plant samples were around 0.9 ng/L and rhizosphere soil was around two times higher which was more than 2 ng/g (Table 4). The high concentration of PFOS was only detected in the water samples but not in sediment or the plant samples nearby. The water sample we collected was surface water.

Table 4: PFAS Concentration in Ringwood Samples

	PFOS	**PFOA**	**PFNA**
Water (ng/L)	445.56	23.78	25.69
Sediments (ng/g)	0.71-1.14	0.43-0.45	n.d.
Plant-Jewelweed (ng/g)			
Rhizosphere Soil	2.17-2.30	0.34-0.66	n.d.
Root	0.811	2.121	n.d.
Shoot	0.73-0.97	1.00-1.22	n.d.

Table 5 shows PFAS concentration in water, sediment and plant samples in Battlefield Park. The highest concentration PFAS in water (pH=7.25) was PFNA (16.75 ng/L), which was higher than the maximum contaminant level (MCL=13 ng/L PFNA) in drinking water of New Jersey. The lower concentration of PFAS in water and sediment could not be used to conclude the effluent from the factory is clean, considering the large volume of Delaware River and the far distance between sampling point and factory could contribute to the dilution of PFAS concentration. The sediment and soil collected from this location were very sandy with larger particle size and low sticky lumps, which might have low retaining effects on PFAS[59]. Elevated concentrations of PFHxA were measured (1.46 -1.95 ng/g) in the shoot part, while elevated concentrations of PFOS (1.21-1.74 ng/g) were measured in the root samples of grass and purslane plants.

Table 5: PFAS Concentration in Battlefield Park Samples

	PFBS	**PFHpA**	**PFHxA**	**PFHxS**	**PFNA**	**PFOA**	**PFOS**
Water (ng/L)	3.26	1.82	3.76	0.63	16.75	6.37	8.30
Sediments (ng/g)	n.d.	n.d.	n.d.	n.d.	0.09-0.15	n.d.	0.07-0.10
Plant 1-Carex viridula Michx(ng/g)							
Nearly Soil	n.d.	n.d.	n.d.	n.d.	0.11-0.13	n.d.	0.070-0.15
Rhizosphere Soil	n.d.	n.d.	0.15-0.18	n.d.	0.144-0.18	n.d.	0.15-0.19
Root	n.d.	n.d.	0.997	n.d.	0.84	n.d.	1.21
shoot	n.d.	n.d.	1.81-1.95	n.d.	0.11-0.19	n.d.	0.67-0.48
Plant 2-Ludwigia palustris (Water Purslane) (ng/g)							
Nearly Soil	n.d.	n.d.	n.d.	n.d.	0.08-0.11	n.d.	0.09-0.12

Rhizosphere Soil	n.d.	n.d.	n.d.	n.d.	0.06-0.086	n.d.	0.05-0.07
Root	n.d.	n.d.	1.42	n.d.	1.7	n.d.	1.74
shoot	n.d.	n.d.	1.46-1.85	n.d.	0.42-0.73	n.d.	0.33-00.83
Plant 3-Eupatorium serotinum Michx(ng/g)							
Rhizosphere Soil	n.d.	n.d.	n.d.	n.d.	n.d.	n.d.	0.12-0.20
Root	n.d.	n.d.	n.d.	n.d.	n.d.	n.d.	0.19-0.22
Young Stem	n.d.	n.d.	0.41-0.51	n.d.	0.06-0.07	n.d.	0.11-0.19
Young Leaves	n.d.	n.d.	0.33	n.d.	0.29-0.32	n.d.	0.78-1.01
Old Stem	n.d.	n.d.	0.18-0.20	n.d.	n.d.	n.d.	0.11-0.13
Old Leaves	n.d.	n.d.	0.29	n.d.	0.33-0.53	n.d.	0.60-0.73

Little Pine Lake was the location where the highest total PFAS concentration in fish samples of one NJDEP project in 2019 was found.[52] The samples were collected from the main lake (Table 6 (a), pH=6.25) and a tributary (Table 6 (b), pH=5.94) on the north of the river. The PFAS concentrations in tributaries (moving water: PFHxA 24.64-28.79 ng/L, PFOA 17.68-19.41 ng/L, PFHxS 54.29-64.18 ng/L, PFOS 22.32-23.24 ng/L, stagnant water: PFHxA 19.32-19.45 ng/L, PFOA 11.28-11.81 ng/L, PFHxS 19.95-27.44 ng/L, PFOS 1.97-11.59 ng/L) were higher than those samples collected in the main lake where all PFAS concentration were lower than 13 ng/L. With high concentrations in water samples, PFHxS were firstly found highly accumulated in one plant root and its rhizosphere soil samples (plant 3 *Juncus articulatus L.* sampled near bridge of the tributaries, 1.92-1.96 ng/g in rhizosphere soil and 2.21-2.3 ng/g in root). PFOS was measured at high concentrations in all rhizosphere soils in both locations (1.21 ng/g to 11.82 ng/g) and three root samples (1.64 - 2.12 ng/g of the *riverbank sedge* near lake, 12.34-13.91 ng/g of *Chamaedaphne calyculata (L.) Moench* and 22.49-24.59 ng/g of *Juncus articulatus L.* near tributaries). Two shoot parts of plant samples were detected with high concentration of PFHxA (1.16-1.5 ng/g) near the tributaries.

Table 6 (a): PFAS Concentration in Little Pine Lake- Lake Samples

	PFBS	**PFHpA**	**PFHxA**	**PFHxS**	**PFNA**	**PFOA**	**PFOS**
Water (ng/L)	0.50-0.58	0.63-1.18	1.62-3.19	1.49-2.24	0.61-1.11	4.28-3.69	7.52-11.33
Sediments (ng/g)	n.d.	0.15	0.11-0.16	0.51-0.69	n.d.	n.d.	1.34-1.50
Plant1-Xylosma flexuosa (Kunth) Hemsl(ng/g)							
Rhizosphere soil	n.d.	n.d.	n.d.	n.d.	n.d.	n.d.	2.62-2.71
Root	n.d.	n.d.	n.d.	n.d.	n.d.	n.d.	0.67-0.87
Stem	n.d.	n.d.	0.46-0.60	n.d.	n.d.	n.d.	n.d.
Leaves	n.d.	n.d.	0.32	n.d.	n.d.	n.d.	n.d.
Plant2- Alnus serrulata (Aiton) Willd (ng/g)							
Rhizosphere soil	n.d.	0.14-0.19	0.16-0.17	0.14-0.17		0.19-0.3	4.22-4.34
Root	n.d.	0.22-0.27	n.d.	n.d.	n.d.	n.d.	0.40-0.46
Plant 3-Carex emoryi Dewey (Riverbank sedge) (ng/g)							
Rhizosphere soil	n.d.	n.d.	0.21-0.46	0.52-0.73	n.d.	0.27	10.28-11.82
Root	n.d.	1.4-2.37	n.d.	n.d.	n.d.	n.d.	1.64-2.12

shoot	n.d.	n.d.	0.38-0.70	n.d.	n.d.	n.d.	n.d.

Table 6 (b): PFAS Concentration in Little Pine Lake- Bridge Near Tributaries Stream Samples

	PFBS	**PFHpA**	**PFHxA**	**PFHxS**	**PFNA**	**PFOA**	**PFOS**
Moving Water (ng/L)	5.96-7.11	7.50-8.42	24.64-28.79	54.29-64.18	1.98-2.48	17.68-19.41	22.32-23.24
Sediment (ng/g)	n.d.	n.d.	n.d.	0.34-0.35	n.d.	n.d.	1.99-2.14
Stagnant Water (ng/L)	3.60-4.14	5.25-5.54	19.32-19.45	19.95-27.44	1.29-1.41	11.28-11.81	1.97-11.59
Sediment (ng/g)	n.d.	n.d.	n.d.	n.d.	n.d.	n.d.	0.46-0.47
Plant1-Chamaedaphne calyculata (L.) Moench (ng/g)							
Rhizosphere soil	n.d.	0.12	0.16	0.76-0.79	n.d.	0.12	4.7-5.19
Root	n.d.	0.81	0.45-0.68	0.61-1.08	n.d.	n.d.	12.34-13.91
Plant 2-Juncus inflexus L. (ng/g)							
Rhizosphere soil	n.d.	n.d.	0.12	0.28	n.d.	n.d.	1.21
Root	n.d.	n.d.	n.d.	n.d.	n.d.	n.d.	0.45-0.75
shoot	n.d.	n.d.	1.5	n.d.	n.d.	n.d.	n.d.
Plant3-Juncus articulatus L (ng/g)							
Rhizosphere soil	n.d.	0.14-0.27	0.13-0.20	1.92-1.96	n.d.	0.24-0.27	8.22-8.40
Root	n.d.	n.d.	0.53-0.65	2.21-2.3	n.d.	0.24-0.4	22.49-24.59
shoot	n.d.	n.d.	1.16-1.46	0.33-0.39	n.d.	n.d.	0.31

Samples near a landfill in Kearney were collected from two little creeks by the side of the main entrance to the landfill, draining from the landfill (Table 7). Location 1 (L1) water sample (pH=8.18) was collected from one creek with outlets, location 2 (L2) water (pH=7.55) was collected from the creek around 15 m from L1, L1 was closer to the landfill. PFOA and PFOS was measured highest concentrations from both creeks, the PFOA concentration were 51.50-100.27 ng/L in L1 water and 34.50 ng/L to 64.6 ng/L in L2 water, PFOS concentration were 41.21-91.72 ng/L in L1 water and 33.17-45.24 ng/L in L2 water. All sediment and plant samples were collected from location 2, in plant *Rumex crispus L*, PFOA (1.36-2.18 ng/L) and PFOS (9.63-12.89 ng/L) were found high concentration in rhizosphere soil samples, PFOS (1.25-1.56 ng/g) also found high concentration in root samples of one plant; In plant *Phragmites australis,* PFOS was detected high concentrations of rhizosphere soils (5.74-6.49 ng/L) and roots (4.83-6.16 ng/L).

Table 7: PFAS Concentration in NJMC-1-E Landfill Samples

	PFBS	PFHpA	PFHxA	PFHxS	PFNA	PFOA	PFOS
L1-Water (ng/L)	7.23-10.82	6.51-13.77	9.77-20.85	5.62-12.4	3.51-10.30	51.50-100.27	41.21-91.72
L2-Water (ng/L)	7.24-7.95	10.36-10.98	15.30-17.36	7.90-9.33	5.80-7.44	34.50-64.60	33.17-45.24
L2-Sediment (ng/g)	n.d.	0.06	0.09-0.14	n.d.	0.03-0.05	0.40-0.51	3.17-5.79
plant 1-Rumex crispus L. (curly dock) (ng/g)							
Rhizosphere soil	n.d.	0.22-0.3	0.29-0.44	0.17-0.34	n.d.	1.36-2.18	9.63-12.41
Root	n.d.	n.d.	n.d.	0.01-0.04	n.d.	0.03-0.05	1.25-1.56
stem	n.d.	n.d.	0.01	n.d.	n.d.	n.d.	n.d.
leave	n.d.	n.d.	0.01-0.23	n.d.	n.d.	n.d.	n.d.
Plant 2-Rumex crispus L. (curly dock) (ng/g)							
Rhizosphere soil	n.d.	0.13-0.18	0.18-0.26	0.26-0.28	n.d.	1.36-1.72	11.45-12.89
Root	n.d.	n.d.	0.01-0.07	n.d.	n.d.	n.d.	0.33-0.37
stem	n.d.	n.d.	0.01	n.d.	n.d.	n.d.	n.d.
Leaves	n.d.	n.d.	0.01	n.d.	n.d.	n.d.	n.d.
Plant 3-Phragmites australis (ng/g)							
sediment-wetland	n.d.	n.d.	0.12-0.15	n.d.	n.d.	0.5-0.59	5.74-6.49
Rhizosphere soil l	n.d.	n.d.	n.d.	n.d.	n.d.	0.63-0.70	4.83-6.16
shoot	n.d.	n.d.	0.03-0.04	n.d.	n.d.	n.d.	n.d.

Using Nano-ESI-HRMS, chloroperfluoropolyether carboxylates (ClPFPECA) in the extracts from aforementioned soil and plant samples were screened. However, none of these samples showed positive detection of ClPFPECA. This was probably due to the differences in extraction and concentration procedures employed in this study as compared to those in previous publications[6]. Therefore, it is important to optimize the extraction and analytical procedures for the analysis of ClPFPECA in environmental samples for future studies.

Water and sediments from the Passaic River across the Riverside Superfund Site were collected in September 2021. The summary of the results is presented in Table 8.

Table 8: PFAS Concentration in Passaic River Samples

	PFBS	PFHpA	PFHxA	PFHxS	PFNA	PFOA	PFOS
Water (ng/L)	3.21	3.23	5.25	2.77	1.91	14.14	19.11
Sediment 1 (ng/kg)	6.49	0.00	60.49	169.18	47.46	176.04	610.81
Sediment 2 (ng/kg)	12.64	0.00	83.63	0.00	45.31	191.03	591.73

Task 3: Evaluation of PFAS Bioaccumulation by Plants

Project Design and Methods Quality Assurance

The bioconcentration factor (BF) can be used to evaluate the content of PFAS of plant update, which defined as the ratio of the PFAS concentration in root (ng/g dry weight) over the concentration of PFOA in rhizosphere soil (ng/g dry weight, Eq 1), and the translocation factor (TF) can be used to measure the amount of PFAS transferred from one organ to another, which defined as the ratio of the PFAS concentration in shoot over the concentration in root (Eq 2)[57-58]. Thus, BF reflects PFAS plant uptake from the environment, while TF reveals the transport of PFAS within the plant, from root to shoot.

Results and Discussion

BF and TF of different PFAS were calculated by measurable concentration in plant and rhizosphere soil samples (results in Tables 5-7) and shown in Table 9. The level of detection is limited by the extraction efficiency, with the detection limit being the same for all samples once they are processed. Extraction efficiency from plants is very difficult to assess, especially from field plants.

PFBS was primarily detected in water and not found in other samples. PFHxA was detected in most shoots of the plant sample, but not detected in the root samples. The translocation factor of PFHxA were all >1 on the plants that have PFHxA detected both in roots and shoots samples. For example, the TF was 1.78-2.75 of plant *Juncus articulatus* L. in Little Pine Lake wetland location, TF=1.02-1.95 of two plants in Battlefield Park and TF=1-2 of plant *Rumex crispus* L in Kearney landfill location. More PFHxA (6-carbon) translocated from roots to shoots and accumulated more in shoot compared to root. PFNA (9-carbon) as longer chain PFAAs with lower TF (only two plants in Battlefield Park with TF=0.13-0.23 and TF=0.25-0.43) accumulated more in roots compared to shoots. The only TF of PFHxS (6-carbon) obtained in this study was 0.14-0.18, which is higher than the TF value (TF=0.01) of PFOS (8-carbon) within the same plant. With same functional group as PFAS, the shorter chain translocates more from root to shoot. Similar findings by Zhang et al. [60] showed TF values of PFAAs increased with decreasing carbon chain length in *Juncus effusus*. Most TF values of PFOS are 0.01, 0.19-0.48. 0.26-0.59 and 0.40-0.56 and shows that PFOS accumulated more in roots compared to shoots, which is similar to our study

with *Arabidopsis thaliana.* The only plant that was an exception with high TF values of PFOS ranging 4.06-6.37 was a bigger plant (*Eupatorium serotinum Michx*) like a small tree, and it is hypothesized that with lush leaf system and long-term living, PFOS could eventually translocate from root to shoot, and PFOS equilibrium in the rhizosphere could be affected with lower PFOS concentration in soil, leading to PFOS release from root to the grow media (soil).

The bioaccumulation factor of PFHxA was only able to be calculated for one plant in Kearny Landfill with value of 0.04-0.1, which is 3 to 4 times higher than the BF value of PFOA (BF=0.01-0.04) in the same plant. The range of BF value of PFOA were from 0.01 to 6.24 with different plants and different locations. The BF values of PFNA were considered high which are 4.88-5.99 and 19.8-26.52. The two plants with high BF values of PFNA were all collected in Battlefield Park. The rest of the BF values obtained from these two plants were all PFOS, which are 6.2-8.03 and 24.43-32.27.

PFOS was detected in most of the samples in this study among water, sediment, rhizosphere soil and plant, which was the only containment for which we were able to calculate the BF ranges of all plants, based on the triplicate samples collected. The BF values of PFOS for plants collected in Ringwood (BF=0.36), Little Pine Lake (lake location, BF=0.25-0.33, 0.14-0.21, 0.09-0.11), NJMC1-E-landfill (BF=0.1-0.16, 0.03) were all lower than one; two plants collected from Little Pine Lake (tributary location, BF=2.38-2.96, 2.68-2.99) and two plants collected from Battlefield Park (BF=6.2-8.03, 24.43-32.27) were higher than one. Bioconcentration factors represented here as a range of values denotes the range of results from all duplicate analyses. PFOS BF values lower than one were found in plants collected on the sloped bank near the water. The tributary location of Little Pine Lake was a wetland, where plants root system had more access to the water. *Juncus inflexus* was the only plant with BF value lower than one in this location, the hollow structure may help with avoid containment accumulation. The Battlefield Park sampling location was on the bank of Delaware River, whose soils were very sandy, without clay and organic matters, and thus PFAS were not easy to retain in the soil. *Eupatorium serotinum Michx* was the only plant in this location with BF value lower than one, who was mentioned previously that translocated PFOS to the shoot part. The bioaccumulation of PFOS vary with the environment (soil) of plants growth and plants type.

Table 9:PFAS Bioaccumulation Factors in New Jersey Plants

			PFOS		PFHxA		PFHpA	PFOA	PFNA		PFHxS
			Root-Rhizosphere	Shoot-root	Shoot-root	Root-Rhizosphere	Root-Rhizosphere	Root-Rhizosphere	Root-Rhizosphere	Shoot-root	Shoot-root
Ringwood	Soil slop bank	*Jewelweed*	0.35-0.37	NA	NA	NA	NA	3.21-6.24	NA	NA	NA
Battlefield Park	sandy bank	*Carex*	6.2-8.03	0.40-0.56	1.82-1.95	NA	NA	NA	4.80-5.99	0.13-0.23	NA
		Water Purslane	24.43-32.27	0.19-0.48	1.02-1.31	NA	NA	NA	19.8-26.52	0.25-0.43	NA
		Late boneset	0.96-1.82	4.06-6.37	NA	NA	NA	NA	NA	NA	NA
Little Pine Lake-L1	soil sloped bank	*Xylosma*	0.25-0.33	NA	NA	NA	NA	NA	NA	NA	NA
		Alnus	0.09-0.11	NA	NA	NA	1.16-1.93	NA	NA	NA	NA
		Carex	0.14-0.21	NA	NA	NA	NA`	NA	NA	NA	NA
Little Pine Lake-L2	wetland	*Chamaedaphne*	2.38-2.96	NA	NA	NA	NA	NA	NA	NA	NA
		Juncus inflexus	0.37-0.62	NA	NA	NA	NA	NA	NA	NA	NA
		Jointed Rush	2.68-2.99	0.01	1.78-2.75	NA	NA	0.89-1.67	NA	NA	0.14-0.18
NJMC1-E-Landfill	soil sloped bank	*Rumex crispus* L	0.1-0.16	NA	NA	NA	NA	0.01-0.04	NA	NA	NA
		Rumex crispus L.	0.03	NA	1-2	0.04-0.11	NA	0.01-0.04	NA	NA	NA
	wetland	*Phragmites australis*	NA	NA	NA	NA	NA	NA	NA	NA	NA

PFAS distribution and partition between water and sediment samples

The distribution between PFAS concentration in plants and water and the distribution of PFAS concentration in water and sediment was analyzed for plants that have PFAS with measurable concentrations and it is plotted in Figure 8 (b). PFHpA and PFOA were only found three plants with measurable concentrations, the concentrations of PFHpA accumulated in plants were from 0.25 to 1.89 ng/g with PFHpA in water from 0.91 to 5.4 ng/L. The PFOA concentrations (11.5 to 23.78 ng/L) in water was much higher compared to PFHpA, however, the concentration in plants was not increased from 0.04 ng/g to 3.213 ng/g. The PFHxA concentrations in plants were varies more with location compared the concentration in water, the concentration of plants from the location of water concentration of 3.76 ng/L was 1.27-3.08 ng/g, from water concentration 2.41 ng/L location was 0.54-0.85 ng/L, from water concentration 16.33 ng/L location was 0.04-0.13 ng/g. PFOS was the only contaminant found in all plant samples, the trend of PFOS partition in plant samples and water was not clear. The PFOS concentration in plant samples was 0.43-2.32 ng/g with water concentration 8.3-9.46 ng/L. The PFOS in plant samples was 0.35-1.41 ng/g with 39.21 ng/L in water, however, the concentration in plant samples was 0.60-23.85 ng/g with 6.78 ng/L in near surface water samples. We did not find a clear trend of the partition of the analyzed PFAS in water samples and co-located plant samples, where plants that grow by the waterbody are expected to be exposed through long roots. Plants from most locations growth on the soil, plant uptake water indirectly form the surface water, the concentration of PFAS in plant was not only affect by the nearby surface water concentration, plant type, soil character would all affect it accumulation in plant.

The PFAS partition of water and sediment were plotted in Figure 8 (a), the concentrations of PFAS in sediment were not directly related to the concentration in water. Due to the limited data of measurable concentration in sediment, PFOS was the only PFAS obtained with more than two data points. With the current data we have, the concentration of short- chain PFAS in sediment decreased with its concentration in surface water increased. For example, PFHxA concentration in water ranged from 2.41 to 16.33 ng/L, its concentration in sediment ranged from 0.12 to 0.14 ng/g; PFHxS concentration in water ranged from 1.87 to 59.24 ng/L, its concentration in sediment ranged from 0.60 to 0.35 ng/g; PFHpA concentration in water ranged from 0.91 to 5.40 ng/L, its concentration in sediment ranged from 0.15 to 0.06 ng/g. The 8-carbon PFOA concentration in sediment (0.43 to 0.46 ng/g) positively correlated with its concentration in water (23.78 to 49.55 ng/L), while 9-carbon PFNA did not. Three sample locations showed that the concentration of the 8-carbon PFOS in sediment increased while PFAS concentration in water also increased, whereas the other two sites did not show this correlation.

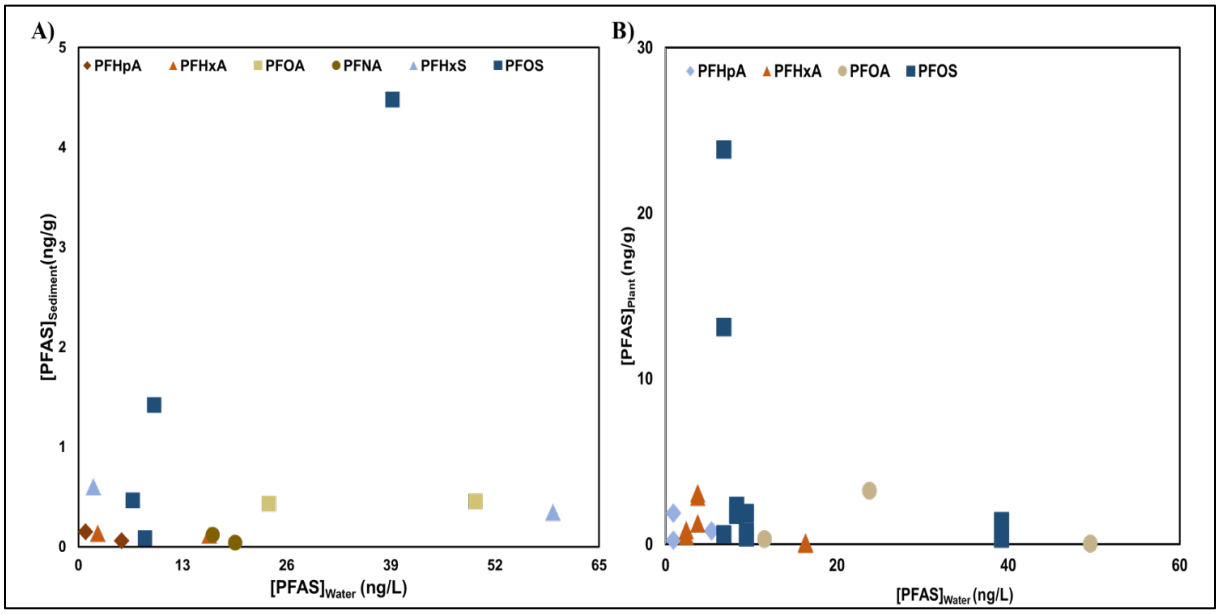

Figure 8: (A) PFAS accumulation in plant and PFAS concentration in water. (B) PFAS partition in water and sediment

PFAS sorption of soil is driven by electrostatic interactions, the negatively charged functional head of PFAS can attracted by the positively charged surfaces adsorbent like oxides, mineral phase, and organic matter[59, 61-62]. Organic matter is known to contribute to PFAS sorption into soil. Total organic carbon in the soil and sediment samples was measured using a total carbon analyzer and the result is shown in Table 10. The soil-water partition coefficient at the various locations was calculated as per equation 3. Previous work from our lab experiment showed the importance of organic carbon of PFAS sorption on soil, however, the concentration in soil samples show little correlation with soil organic carbon, while PFAS molecular weight shows stronger influence on soil adsorption (Figure 9), especially for Little Pine Lake samples. Li et al.[59] investigated factors that influence PFAS sorption and they also found weak correlations between sorption coefficient (K_D) and organic carbon or pH alone, concluded the sorption behavior of PFAS could not be explained by one single sediment property.

Table 10: Total organic concentration and soil-water partition coefficient in the samples

		Kd (L/Kg)					
	TOC (%)	**PFOS**	**PFOA**	**PFNA**	**PFHxS**	**PFHxA**	**PFHpA**
Ringwood	7.97	1.73	18.08	NA	NA	NA	NA
Battlefield Park	1.37	10.24	NA	7.16	NA	NA	NA
Little Pine Lake-L1	20.96	150.66	NA	NA	321.72	56.13	165.75
Little Pine Lake-L2	6.8	68.58	NA	NA	5.82	NA	NA
NJMC1-E-Landfill	1.69	114.27	9.18	6.04	NA	7.04	5.62

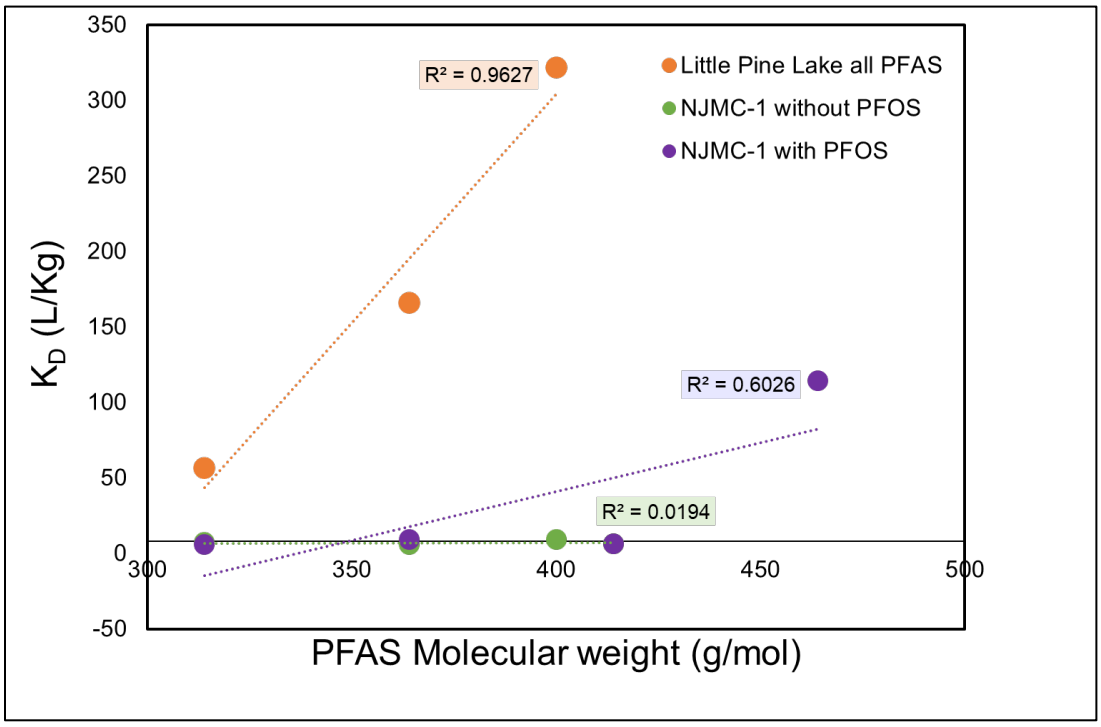

Figure 9 Correlation between soil-water partition coefficient in Little Pine Lake samples and NJMC-1 landfill samples.

Microbe Community Evaluation of soil and plant samples

The microbial community of soil rhizosphere, outside and inside root were evaluated by DNA Illumina sequencing. The DNA was extracted using a soil DNA extraction kit and samples were sent to an external lab for sequencing, then the obtained data was analyzed at the OTU level. The non-metric multi-dimensional scaling (NMDS) plot shows clusters for the microbial communities of the soil rhizosphere, outside of the roots and inside the roots, indicating a higher similarity of the microbial communities within the location in the plant (Figure 10).

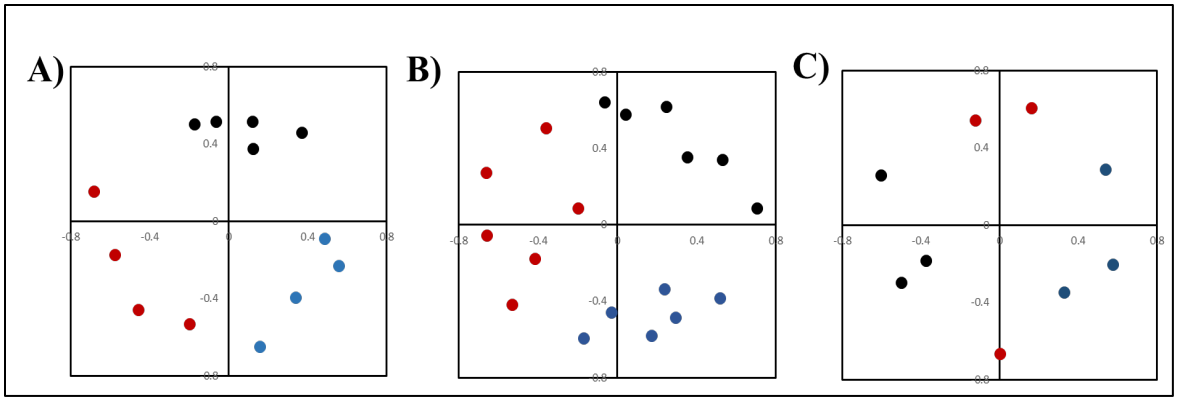

Figure 10 : Non-metric Multi-dimensional Scaling (NMDS) of microbial communities in A) Battlefield Park, B) Location Little Pine Lake-L1 and C) Little Pine Lake-L2, ●Soil rhizosphere, ● Root rhizosphere, ● Root endosphere.

The Shannon index was generated using Mothur (https://mothur.org/wiki/shannon/) and serves as an indicator of the diversity of microbial communities, and it was used to evaluate a correlation between PFAS concentration and microbial diversity. The diversity decreased from outside to inside of the plant, which the most diversity was found in soil rhizosphere, followed with root rhizosphere and root endosphere (Figure 11). The Shannon diversity of the microbial community right outside the root increased with the PFAS concentration in the plant in same location, however, the diversity was not found a trend with sample from mixed locations (Figure 12).

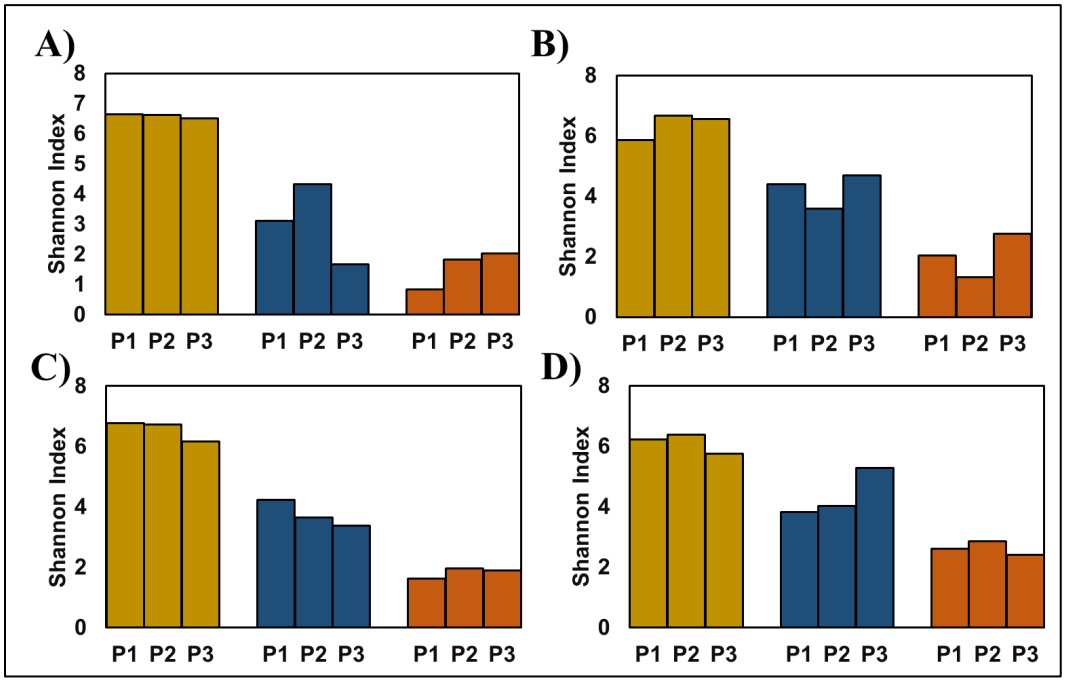

Figure 11: Shannon diversity index of A) Battlefield Park, B) Little Pine Lake-L1, C) Little Pine Lake-L2 and D) NJMC-1 Landfill, ■ Soil, ■ Rhizosphere, ■ Endosphere.

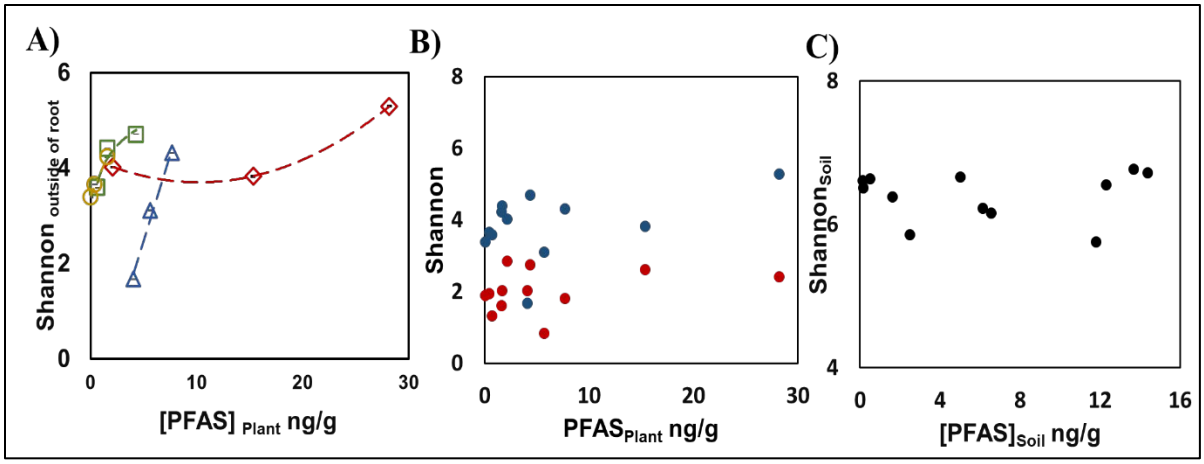

Figure 12: Shannon diversity index with PFAS concentration, A) microbial communities in root rhizosphere (outside of the root) for each location, B) microbial communities in root rhizosphere and root endosphere for mixed locations, C) microbial communities in soil for mixed locations.

Task 4: Biotransformation of PFAS by Soil Bacteria

Background

Rhizospheric bacteria are known to play a pivotal role in PFAS biotransformation and biodefluorination in soils.[63] In this project, we selected *Rhodococcus jostii* RHA1 as a model bacterium, representing bacteria that are ubiquitous and abundant in plant rhizosphere. Here, we investigated the biotransformation of 6:2 fluorotelomer carboxylic acid (6:2 FTCA). The optimal cultivation conditions to promote biodefluorination was determined by the change of the substrate supplement for cultivating RHA1. Degradation pathways were postulated based on the detection of major metabolites. These efforts provided a fundamental understanding of PFAS biotransformation by rhizospheric bacteria and established alignment with their roles in PFAS attenuation in the field.

Project Design and Methods Quality Assurance

Substrate-mediated FTCA Biotransformation. One nutritionally rich medium and 5 compounds were chosen as the carbon sources to study the substrate-mediated FTCA biotransformation, namely Lysogeny broth (LB), glucose, fructose, pyruvate, BuOH, and PrOH. Except for LB, the other 5 compounds served as the sole carbon source for growing *Rhodococcus jostii* RHA1 (RHA1). Biotransformation of FTCAs was tested using resting cells. 6:2 FTCA and 5:3 FTCA stock solutions were prepared from bulk reagent at the concentration of 40 mM in MeOH by weighing, respectively. Three experimental groups, including FTCA treatment, abiotic control, and microbial control, were set for FTCA biotransformation of each carbon source. All

the experimental groups shared the same analytical control. All experimental groups were prepared in triplicates.

RHA1 single colony grown on LB agar plate was picked and inoculated to (a) 100 mL fresh prepared LB medium or (b) 100 mL of freshly prepared ammonium mineral salts (AMS) solution containing one of 5 carbon sources (20 mM). RHA1 was harvested at exponential phase after 40 hours of incubation, followed by washing three times with deionized (DI) water to remove the residual carbon sources and resuspended in DI as a cell stock. The cell stock concentration was measured by OD_{600}. Then, the cell stock was added to a 60 mL serum bottle and diluted with DI water to achieve the final volume of 20 mL with OD = 1.0. For FTCA treatment, 40 μL of FTCA stock solution was spiked in the system to reach the initial concentration of 40 μM. For abiotic control, the cells were autoclaved before spiking 40 μM FTCA. For microbial control, 40 μL of MeOH was spiked in the system. For analytical control, 40 μL of FTCA stock solution was added to 20 mL DI without inoculating cells. All groups were incubated at 30 °C and shaken at 120 rpm. A 3 mL aliquot was collected at selected intervals to measure the free fluoride and FTCA removal.

Enrichment of FTCA Transformation Products (TPs). We designed a TP enrichment protocol to concentrate the potential FTCA TPs and facilitate the chance for the discovery of novel TPs by Nano-ESI-HRMS developed in Task 1. Four experimental groups, including FTCA treatment, abiotic control, analytical control, and microbial control, were set in duplicates.

RHA1 single colony grown on LB agar plate was picked and inoculated to 100 mL of freshly prepared ammonium mineral salts (AMS) solution containing 20 mM glucose. RHA1 was harvested at exponential phase after 40 hours of incubation, followed by washing three times with deionized (DI) water to remove the residual glucose and resuspended in DI as a cell stock. The cell stock concentration was measured by OD_{600}. The cell stock was added to a 60-mL serum bottle and diluted to DI water to achieve the final volume of 15 mL with OD = 1.0. For FTCA treatment, 60 μL of FTCA stock solution was spiked in the system to reach the initial concentration of 80 μM. For abiotic control, the cells were autoclaved before spiking 60 μM FTCA. For microbial control, 80 μL of MeOH was spiked in the system. For analytical control, 60 μL of FTCA stock solution was added to 15 mL DI without inoculating cells. All groups were incubated at 30 °C and shaken at 120 rpm. A 3-mL aliquot was collected at 0h and 40 h to measure fluoride release, determine FTCA removal, and identify TPs by Nano-ESI-HRMS as developed in Task 1.

The remaining liquid from the initial FTCA transformation was collected and centrifuged at 12,000 rpm for 5 min to remove all the biosolids. The supernatant was transferred to a 60 mL serum bottle to start a new round of FTCA biotransformation experiment by RHA1 resting cells. In detail, the cell stock was added to the supernatant, adjusting with DI to reach the final volume of 15 mL with OD = 1.0. Then the bottles were incubated under the same condition as the initial FTCA transformation. The FTCA treatment group underwent one initial FTCA transformation and 6 generations of continuous TP enrichment.

Effects of Metal Cations on RHA1 Biodefluorination. (a) *Defluorination inhibition by varied metal cations.* Harvested RHA1 cells was added to a 160-mL serum bottle, spiked with 80 μM 6:2 FTCA and one of 5 metal cations (Fe^{3+}, Zn^{2+}, Ni^{2+}, Ag^{+}, Cu^{2+}, 10 mM) and adjusted to 20 mL with OD_{600} = 1.0. Positive control was prepared without spiking metal cations as a positive fluoride release reference. (b) *Defluorination inhibition by varied Cu^{2+} concentrations.* Similar resting cell treatments were prepared as (a) by dosing Cu^{2+} at different concentrations (0 μM, 0.1 μM, 1 μM, 10 μM, 12 μM, 25 μM, 50 μM, and 100 μM).

Free Fluoride Analysis. A liquid sample (2.0 mL) was collected and filtered through a 0.22-μm PES membrane. After mixing with 2.0 mL of TISAB II buffer solution (Thermo-Fisher Scientific), fluoride concentration was measured using the Orion Star Meter equipped with the fluoride electrodes (Thermo-Fisher Scientific).

Results and Discussion

Substrate-mediated FTCAs Aerobic Defluorination. Free fluoride release from 6:2 FTCA and 5:3 FTCA using RHA1 resting cells fed with 6 carbon sources are shown in Figure 13. The significant accumulation of free fluoride (18 ~52 μM, Figure 13 a) within 28 h was observed in all six 6:2 FTCA treatments, while no fluoride increase (<1.5 μM) was detected in 5:3 FTCA treatments. The distinctive fluoride release trend between 6:2 FTCA and 5:3 FTCA biotransformation via RHA1 was consistent with our previous observations for activated sludge, which further supported that 6:2 FTCA was biotransformed via fluoride releasing pathways and 5:3 FTCA was biotransformed following non-fluoride releasing pathways.

For 6:2 FTCA treatments, the fluoride release was initiated as soon as the experiments began, and the fluoride accumulation rate slowed down, reaching a platform after 10 h, except for pyruvate grown RHA1. When grown with different carbon sources, RHA1 presented various fluoride release capacities and rates (Figure 13). The fluoride release capacities were ranked as glucose (52 μM) ≈ fructose (50 μM) > LB (34 μM) ≈ 1-butanol (BuOH) (30 μM) ≈ 1-propanol (PrOH) (27 μM) > pyruvate (18 μM) based on the accumulated fluoride at the end of experiments (28 h). A similar rank trend was shown for fluoride release rates when the average fluoride accumulation per hour was computed based on the results in the first 10 hours. Considering the identical initial biomass (OD600 = 1.0), the varied fluoride release capacities and rates suggested that defluorination of 6:2 FTCA by RHA1 was substrate-mediated, and different carbon sources can lead to the different expression levels for defluorinating enzymes.

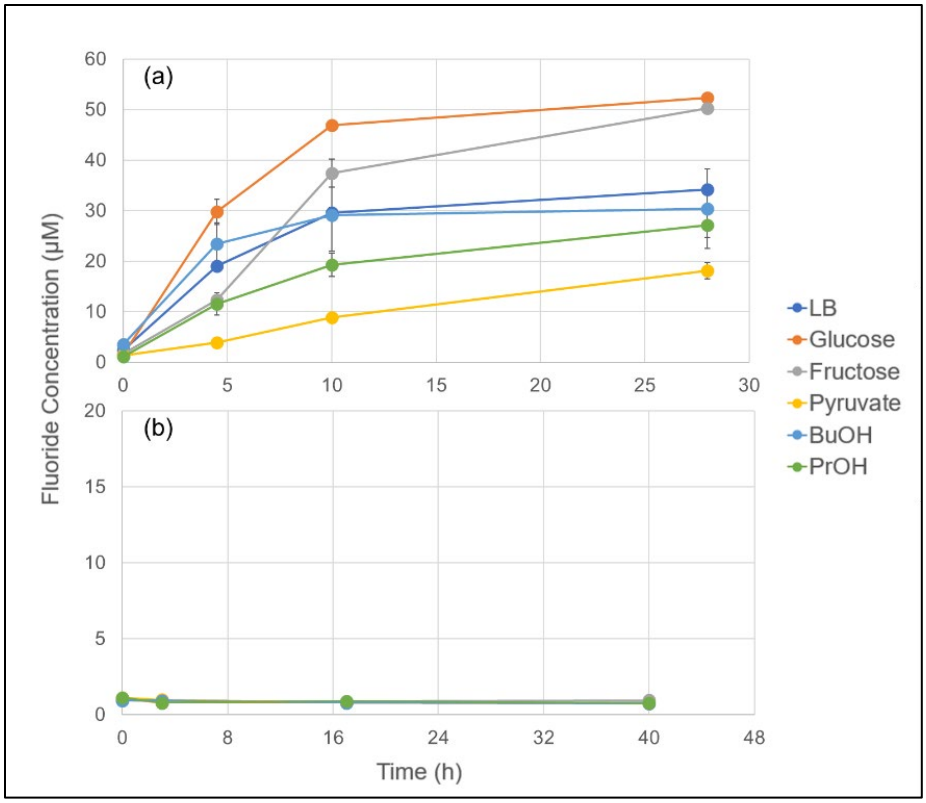

Figure 13: Fluoride release of (a) 6:2 FTCA and (b) 5:3 FTCA by Rhodococcus jostii RHA1 grown with 6 different carbon sources. Note that in Figure b, there was no fluoride across these six treatments, therefore all the lines are stacked.

Novel 6:2 FTCA Biotransformation Products by *Rhodococcus jostii* RHA1. To concentrate and identify the novel major biotransformation products (TPs), TP enrichment experiments were conducted when RHA1 resting cells were exposed to 6:2 FTCA. For 6:2 FTCA TP enrichment samples, continuous fluoride accumulation was observed over 7 generations of reactions (Figure 14), with complete removal of spiked 6:2 FTCA in each round (Figure 15). The average numbers of fluoride release per 6:2 FTCA molecule of 1st – 7th generation reactions were 0.71, 0.71, 2.26, 1.37, 1.93, 1.63, 2.46, suggesting the presence of fluoride and the accumulation of TPs were not hindering the biotransformation and biodefluorination process of 6:2 FTCA.

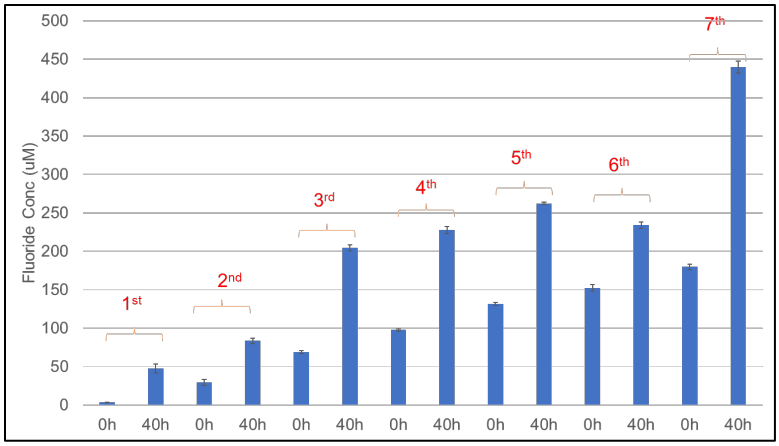

Figure 14: The concentration of free fluoride at time 0h and 40h in 7 generations of 6:2 FTCA TPs enrichment experiments.

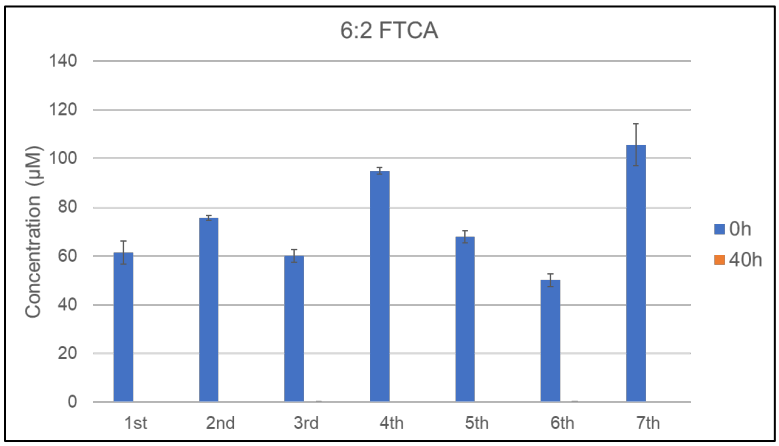

Figure 15: 6:2 FTCA removal at 0 h and 40 h in 7 generations of 6:2 FTCA TP enrichment experiments. Note that the concentration at 40 h is just above or below detection at each generation.

With non-target analysis, one important anion (m/z = 696.20) was found as the 6:2 FTCA TP candidate (Figure 16). As shown in Figure 16, the occurrence of daughter peaks at m/z = 292.98 ($C7F11^-$) and at m/z = 356.98 ($C8F12HO2^-$, 6:2 FTUCA) in the MS/MS spectrum indicates the anion at m/z = 696.20 is a fluorine-containing compound and of high chance a conjugation of 6:2 FTUCA. The anion at m/z = 696.20 was possibly a biotransformation intermediate after one fluorine was released from the 6:2 FTCA molecule.

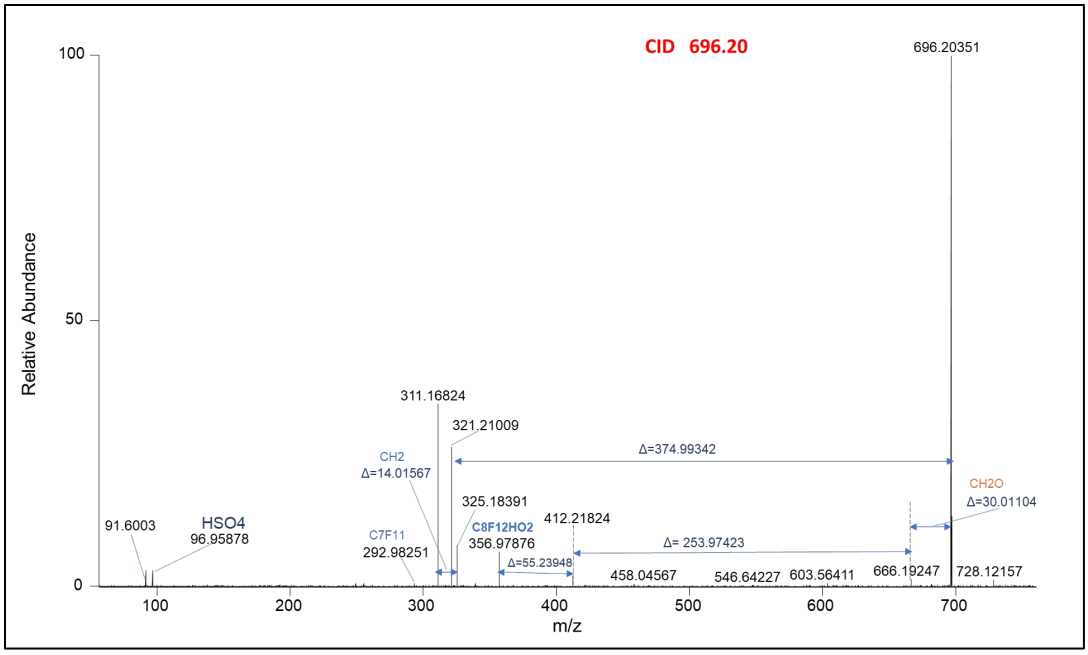

Figure 16: MS/MS CID spectrum of m/z=696.20, a suspect 6:2 FTCA TP in RHA1.

Effect of Heavy Metals on 6:2 FTCA Defluorination. Free fluoride release is a direct and important sign of 6:2 FTCA biodefluorination, within limits reflecting the activity and extent of 6:2 FTCA biotransformation. Therefore, different experiments were carried out to investigate the influencing factors for free fluoride release in 6:2 FTCA biotransformation. Heavy metals were commonly known for their inhibition effects on the bacterial functional enzymes or the biodegradation of contaminants. Five heavy metal ions (Fe^{3+}, Zn^{2+}, Ni^{2+}, Ag^{+}, Cu^{2+}) were selected in this study. For example, Ni^{2+} and Cu^{2+} seriously inhibited phenol degradation by *Rhodococcus sp.* strain P1[64]. Ni^{2+} and Zn^{2+} inhibited the alkylbenzene removal by *Bacillus* strain[65]. Cu^{2+} and Ag^{+} were found to reduce the fluorobenzene biodegradation and inhibit the fluoride release by *Labrys portucalensis*[66]. Iron (Ferric) was reported to inhibit the perchlorate biodegradation[67] and the activity of cellulases[68].

As shown in Figure 17, 5 heavy metal ions all caused significant reduction of fluoride release when compared with positive control. In detail, the fluoride release reduced by 94.6% for Fe^{3+}, 89.2% for Zn^{2+}, 98.4% for Ag^{+}, 66.3% for $Ni^{2+,}$ and 98.4% for Cu^{2+}, following the rank of $Ag^{+} \approx Cu^{2+} > Fe3^{+} > Zn2^{+} > Ni^{2+}$ (Figure 12a). Notably, only about 5% (3.7 ~ 6.3 μM) of the spiked 6:2 FTCA was detected in Fe^{3+} treatment from 0 h to 40 h, indicating that 100 μM Fe^{3+} may form conjugates with 6:2 FTCA (Figure 12b). The removal of 6:2 FTCA was compatible with the fluoride release trend. 6:2 FTCA removal was only observed in Ni^{2+} treatment (28.7%), while that was negligible in other metal treatments. The addition of Ni^{2+} did not stoichiometrically affect the fluoride release compared to the positive control.

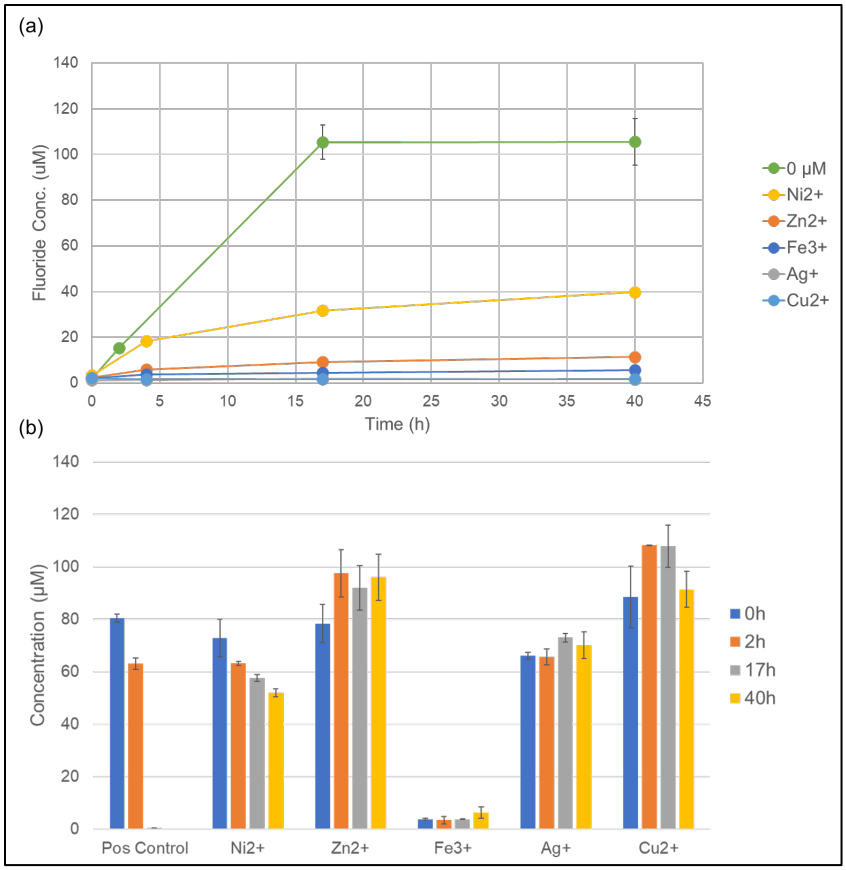

Figure 17: Fluoride release (a) and 6:2 FTCA concentration (b) in positive control and 5 metal cation treatments of 6:2 FTCA biotransformation by RHA1.

The inhibition effect of Cu^{2+} on 6:2 FTCA degradation and defluorination was negligible when the dosage was equal to or smaller than 1 µM (Figure 18 and Figure 19). Meanwhile, the 6:2 FTCA degradation and defluorination were completely inhibited when the Cu^{2+} dosage was equal to or above 25 µM (Figure 18 and Figure 19). Moderate fluoride release (35.1~37.9 µM) was observed at the dosage of 10 and 12 µM corresponding with the 6:2 FTCA removal following the same stoichiometric as the positive control. Interestingly, the accumulation of 6:2 FTUCA at 17 and 40 h were observed in the treatments with 10~100 µM of Cu^{2+} dosage when 6:2 FTCA degradation and defluorination were inhibited. Meanwhile, 6:2 FTUCA in 0.1 and 1 µM Cu^{2+} treatments fully vanished after 17 h as the positive control. Hence, the Cu^{2+} may inhibit the fluoride release by hindering the further biotransformation of 6:2 FTUCA.

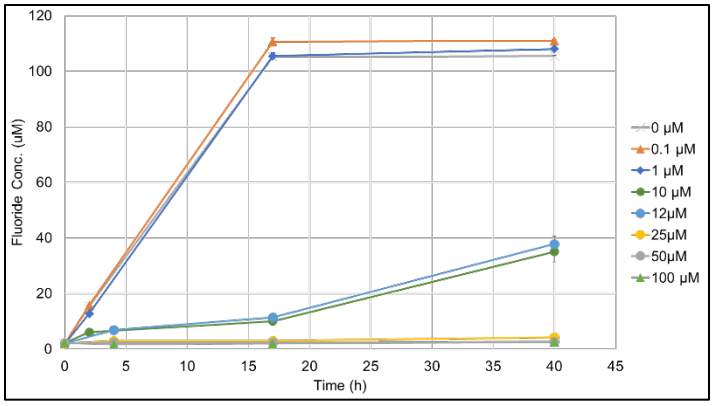

Figure 18: Fluoride release of eight 6:2 FTCA treatments spiking with varied Cu^{2+} (aq) concentrations.

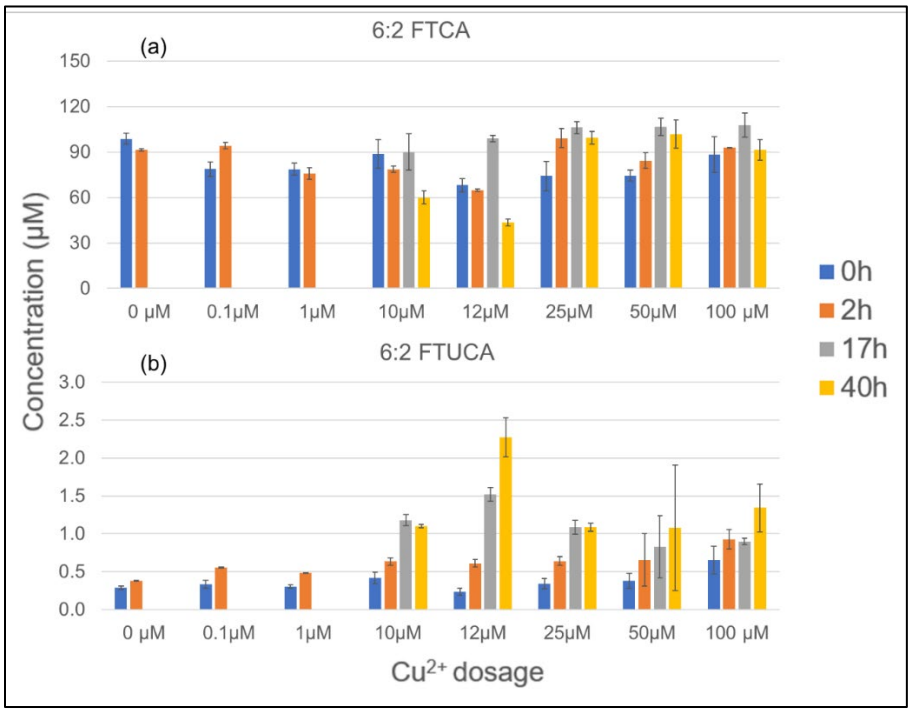

Figure 19: The concentration of (a) 6:2 FTCA and (b) 6:2 FTUCA of eight 6:2 FTCA treatments spiking with varied Cu^{2+} (aq) concentrations.

Conclusions and Recommendations for Future Research and Application and Use by NJDEP

In this study, we developed a rapid analytical method for PFAS combining nano-electrospray ionization and high-resolution mass spectrometry (Nano-ESI-HRMS). This method exhibited high sensitivity with LODs of 3.2~36.2 ng/L for 22 target PFAS analytes. In AFFF formulations, Nano-ESI-HRMS enabled the first-time detection of less-fluorinated 5:3 FTUCA as a novel biotransformation metabolite by activated sludges collected in New Jersey. Further, Nano-ESI-HRMS enabled comprehensive PFAS quantitative analysis and suspect screening, applicable for rapid investigation and assessment of PFAS-related exposure and treatment in environmental matrixes. Thus, this project enabled the establishment of a standard operating procedure (SOP) for PFAS analysis by this newly developed Nano-ESI-HRMS available to NJDEP and other parties of interest.

Surveys in water, sediment, and plants from four sites in New Jersey revealed a ubiquitous PFAS contamination issue particularly in proximity of landfills. The highest PFAS concentration in surface water was found near the Ringwood Superfund site downstream a waste disposal area on a foamy stream (PFOS 445.56 ng/L), and highest sediment concentration was found near the landfill in Kearny (PFOS 3.17-5.79 ng/g). PFOS was detected in most soil and sediment samples with measurable concentration compared to the other PFAS that were not measured in the collected sediment or plant samples.

Bioaccumulation of PFOS in plants was relatively high in Little Pine Lake (PFOS 22.79-24.90 ng/g) and it was measured in all the collected samples, indicating a widespread occurrence. Perfluorohexanoic acid (PFHxA) was primarily detected in shoot samples of plants, suggesting the translocation of this PFAS from the environment. However, the PFAS concentration in water and its concentration in near environmental media are poorly correlated, considering the properties of sediments and type of plants varies from location to location.

Though perfluorinated chemicals like PFOS and PFOA are widely considered “nonbiodegradable”, polyfluorinated chemicals like 6:2 FTCA and 6:2 FTS can be biotransformed and even biodefluorinated. Understanding biodefluorination is important as it catalyzes the cleavage of the highly stable C-F bonds and liberate F from PFAS molecules. Our study focused on the biotransformation of 6:2 FTCA by the bacterium RHA1, a catabolic powerhouse. Sustainable biodefluorination of 6:2 FTCA was observed with the release of free fluoride. With non-target analysis by Nano-ESI-HRMS, a 6:2 FTUCA conjugate was identified as a major transformation product, supporting the existence of biodefluorination. In contrast, minimal fluoride release was consistently observed during 5:3 FTCA biotransformation. Low detection of less fluorinated 5:3 FTUCA and PFBA may explain the minimal fluoride release, demonstrating the minor contribution of well-received fluoride-releasing pathways.

Based on these key findings of this study, we outline several key observations that can be beneficial to NJDEP.

(1) Except PFOS, PFOA, and other target PFAS, there exist many other PFAS that are not targeted by the EPA standard methods in the environment.[2, 6, 8, 69-71] Nano-ESI-HRMS and other approaches (e.g., TOP assay) can be important to gain a comprehensive view of PFAS contamination to characterize the sources (e.g., storm water) and understand their attenuation and fate in the environment.
(2) Landfill sites can be of significant concern given the high concentration of PFAS detected in water and sediment.
(3) Plants can accumulate and translocate PFAS to edible parts (e.g., shoot and leaves). Through consumption, PFAS can enter the food web and accumulate in biota.
(4) Biodefluorination is a green way to eliminate PFAS for sustainable remediation and management. Our studies provided lines of evidence showing the ability of RHA1 for biodefluorination though its molecular foundation requires future efforts for characterization.

References

1. Wu, C.; Goodrow, S.; Chen, H.; Li, M., Distinctive biotransformation and biodefluorination of 6:2 versus 5:3 fluorotelomer carboxylic acids by municipal activated sludge. *Water Research* **2024,** *254*, 121431.
2. Wu, C.; Wang, Q.; Chen, H.; Li, M., Rapid quantitative analysis and suspect screening of per-and polyfluorinated alkyl substances (PFASs) in aqueous film-forming foams (AFFFs) and municipal wastewater samples by Nano-ESI-HRMS. *Water Research* **2022,** *219*, 118542.
3. Barzen-Hanson, K. A.; Roberts, S. C.; Choyke, S.; Oetjen, K.; McAlees, A.; Riddell, N.; McCrindle, R.; Ferguson, P. L.; Higgins, C. P.; Field, J. A., Discovery of 40 Classes of Per- and Polyfluoroalkyl Substances in Historical Aqueous Film-Forming Foams (AFFFs) and AFFF-Impacted Groundwater. *Environmental Science & Technology* **2017,** *51* (4), 2047-2057.
4. Johnson, M. S.; Buck, R. C.; Cousins, I. T.; Weis, C. P.; Fenton, S. E., Estimating Environmental Hazard and Risks from Exposure to Per‐ and Polyfluoroalkyl Substances (PFAS): Outcome of a SETAC Focused Topic Meeting. *Environmental Toxicology and Chemistry* **2020**.
5. Buck, R. C.; Franklin, J.; Berger, U.; Conder, J. M.; Cousins, I. T.; de Voogt, P.; Jensen, A. A.; Kannan, K.; Mabury, S. A.; van Leeuwen, S. P., Perfluoroalkyl and polyfluoroalkyl substances in the environment: terminology, classification, and origins. *Integrated environmental assessment and management* **2011,** *7* (4), 513-541.
6. Washington, J. W.; Rosal, C. G.; McCord, J. P.; Strynar, M. J.; Lindstrom, A. B.; Bergman, E. L.; Goodrow, S. M.; Tadesse, H. K.; Pilant, A. N.; Washington, B. J., Nontargeted mass-spectral detection of chloroperfluoropolyether carboxylates in New Jersey soils. *Science* **2020,** *368* (6495), 1103-1107.
7. Lang, J. R.; Allred, B. M.; Field, J. A.; Levis, J. W.; Barlaz, M. A., National estimate of per-and polyfluoroalkyl substance (PFAS) release to US municipal landfill leachate. *Environmental science & technology* **2017,** *51* (4), 2197-2205.
8. Liu, Y.; D'Agostino, L. A.; Qu, G.; Jiang, G.; Martin, J. W., High-resolution mass spectrometry (HRMS) methods for nontarget discovery and characterization of poly-and per-fluoroalkyl substances (PFASs) in environmental and human samples. *TrAC Trends in Analytical Chemistry* **2019**.
9. EPA, Method 537.1: Determination of Selected Per- and Polyfluorinated Alkyl Substances in Drinking Water by Solid Phase Extraction and Liquid Chromatography/Tandem Mass Spectrometry (LC/MS/MS). **2018**.
10. EPA, Method 1633: Analysis of Per- and Polyfluoroalkyl Substances (PFAS) in Aqueous, Solid, Biosolids, and Tissue Samples by LC-MS/MS. **2021**.
11. Gremmel, C.; Fromel, T.; Knepper, T. P., HPLC-MS/MS methods for the determination of 52 perfluoroalkyl and polyfluoroalkyl substances in aqueous samples. *Anal Bioanal Chem* **2017,** *409* (6), 1643-1655.
12. Coggan, T. L.; Anumol, T.; Pyke, J.; Shimeta, J.; Clarke, B. O., A single analytical method for the determination of 53 legacy and emerging per- and polyfluoroalkyl substances (PFAS) in aqueous matrices. *Analytical and Bioanalytical Chemistry* **2019,** *411* (16), 3507-3520.
13. Luo, Y.-S.; Aly, N. A.; McCord, J.; Strynar, M. J.; Chiu, W. A.; Dodds, J. N.; Baker, E. S.; Rusyn, I., Rapid Characterization of Emerging Per- and Polyfluoroalkyl Substances in Aqueous Film-Forming Foams Using Ion Mobility Spectrometry–Mass Spectrometry. *Environmental Science & Technology* **2020,** *54* (23), 15024-15034.
14. Mulabagal, V.; Liu, L.; Qi, J.; Wilson, C.; Hayworth, J. S., A rapid UHPLC-MS/MS method for simultaneous quantitation of 23 perfluoroalkyl substances (PFAS) in estuarine water. *Talanta* **2018,** *190*, 95-102.
15. Boiteux, V.; Bach, C.; Sagres, V.; Hemard, J.; Colin, A.; Rosin, C.; Munoz, J.-F.; Dauchy, X., Analysis of 29 per- and polyfluorinated compounds in water, sediment, soil and sludge by liquid chromatography–tandem mass spectrometry. *International Journal of Environmental Analytical Chemistry* **2016,** *96* (8), 705-728.
16. Ruyle, B. J.; Pickard, H. M.; LeBlanc, D. R.; Tokranov, A. K.; Thackray, C. P.; Hu, X. C.; Vecitis, C. D.; Sunderland, E. M., Isolating the AFFF Signature in Coastal Watersheds Using Oxidizable PFAS Precursors and Unexplained Organofluorine. *Environmental Science & Technology* **2021,** *55* (6), 3686-3695.
17. Bertrand, R., Quantitative and Qualitative LC-High-Resolution MS: The Technological and Biological Reasons for a Shift of Paradigm. **2018**.
18. Enaksha, R. W.; Gurkeerat, S.; Bradley, L. A.; Todd, A. G.; Ajai, K. C., A Review of Nanoelectrospray Ionization Applications for Drug Metabolism and Pharmacokinetics. *Current Drug Metabolism* **2006,** *7* (8), 913-928.
19. Karas, M.; Bahr, U.; Dülcks, T., Nano-electrospray ionization mass spectrometry: addressing analytical problems beyond routine. *Fresenius' Journal of Analytical Chemistry* **2000,** *366* (6), 669-676.
20. Wilm, M.; Mann, M., Analytical properties of the nanoelectrospray ion source. *Analytical chemistry* **1996,** *68* (1), 1-8.

21. Wang, X.; Yu, N.; Qian, Y.; Shi, W.; Zhang, X.; Geng, J.; Yu, H.; Wei, S., Non-target and suspect screening of per- and polyfluoroalkyl substances in Chinese municipal wastewater treatment plants. *Water Research* **2020,** *183*, 115989.
22. Place, B. J.; Field, J. A., Identification of novel fluorochemicals in aqueous film-forming foams used by the US military. *Environmental science & technology* **2012,** *46* (13), 7120-7127.
23. Strynar, M.; Dagnino, S.; McMahen, R.; Liang, S.; Lindstrom, A.; Andersen, E.; McMillan, L.; Thurman, M.; Ferrer, I.; Ball, C., Identification of novel perfluoroalkyl ether carboxylic acids (PFECAs) and sulfonic acids (PFESAs) in natural waters using accurate mass time-of-flight mass spectrometry (TOFMS). *Environmental science & technology* **2015,** *49* (19), 11622-11630.
24. Wang, Y.; Yu, N.; Zhu, X.; Guo, H.; Jiang, J.; Wang, X.; Shi, W.; Wu, J.; Yu, H.; Wei, S., Suspect and nontarget screening of per-and polyfluoroalkyl substances in wastewater from a fluorochemical manufacturing park. *Environmental science & technology* **2018,** *52* (19), 11007-11016.
25. Liu, Y.; Pereira, A. D. S.; Martin, J. W., Discovery of C5–C17 poly-and perfluoroalkyl substances in water by in-line SPE-HPLC-Orbitrap with in-source fragmentation flagging. *Analytical chemistry* **2015,** *87* (8), 4260-4268.
26. Gago-Ferrero, P.; Schymanski, E. L.; Bletsou, A. A.; Aalizadeh, R.; Hollender, J.; Thomaidis, N. S., Extended Suspect and Non-Target Strategies to Characterize Emerging Polar Organic Contaminants in Raw Wastewater with LC-HRMS/MS. *Environmental Science & Technology* **2015,** *49* (20), 12333-12341.
27. Barzen-Hanson, K. A.; Roberts, S. C.; Choyke, S.; Oetjen, K.; McAlees, A.; Riddell, N.; McCrindle, R.; Ferguson, P. L.; Higgins, C. P.; Field, J. A., Discovery of 40 classes of per-and polyfluoroalkyl substances in historical aqueous film-forming foams (AFFFs) and AFFF-impacted groundwater. *Environmental science & technology* **2017,** *51* (4), 2047-2057.
28. D'Agostino, L. A.; Mabury, S. A., Identification of Novel Fluorinated Surfactants in Aqueous Film Forming Foams and Commercial Surfactant Concentrates. *Environmental science & technology* **2013,** *48* (1), 121-129.
29. Trier, X.; Granby, K.; Christensen, J. H., Polyfluorinated surfactants (PFS) in paper and board coatings for food packaging. *Environmental Science and Pollution Research* **2011,** *18* (7), 1108-1120.
30. Johnson, A. R.; Carlson, E. E., Collision-Induced Dissociation Mass Spectrometry: A Powerful Tool for Natural Product Structure Elucidation. *Analytical Chemistry* **2015,** *87* (21), 10668-10678.
31. Pérez-Ortega, P.; Lara-Ortega, F. J.; García-Reyes, J. F.; Gilbert-López, B.; Trojanowicz, M.; Molina-Díaz, A., A feasibility study of UHPLC-HRMS accurate-mass screening methods for multiclass testing of organic contaminants in food. *Talanta* **2016,** *160*, 704-712.
32. Fornal, E., Study of collision-induced dissociation of electrospray-generated protonated cathinones. *Drug Testing and Analysis* **2014,** *6* (7-8), 705-715.
33. Cooks, R. G., Special feature: Historical. Collision‐induced dissociation: Readings and commentary. *Journal of Mass spectrometry* **1995,** *30* (9), 1215-1221.
34. Zhang, G.; Pan, Z.; Wu, Y.; Shang, R.; Zhou, X.; Fan, Y., Distribution of Perfluorinated Compounds in Surface Water and Soil in Partial Areas of Shandong Province, China. *Soil and Sediment Contamination: An International Journal* **2019,** *28* (5), 502-512.
35. Zhang, W.; Cao, H.; Liang, Y., Plant uptake and soil fractionation of five ether-PFAS in plant-soil systems. *Science of The Total Environment* **2021,** *771*, 144805.
36. USEPA, Method 537.1: Determination of Selected Per- and Polyfluorinated Alkyl Substances in Drinking Water by Solid Phase Extraction and Liquid Chromatography/Tandem Mass Spectrometry (LC/MS/MS). U.S. Environmental Protection Agency, O. o. R. a. D., National Center for Environmental Assessment, Ed. 2018.
37. Liu, N.; Wu, C.; Lyu, G.; Li, M., Efficient adsorptive removal of short-chain perfluoroalkyl acids using reed straw-derived biochar (RESCA). *Science of The Total Environment* **2021,** *798*, 149191.
38. Manicke, N. E.; Abu-Rabie, P.; Spooner, N.; Ouyang, Z.; Cooks, R. G., Quantitative Analysis of Therapeutic Drugs in Dried Blood Spot Samples by Paper Spray Mass Spectrometry: An Avenue to Therapeutic Drug Monitoring. *Journal of The American Society for Mass Spectrometry* **2011,** *22* (9), 1501-1507.
39. USEPA, Detection Limit/Quantitation Limit Summary Table. USEPA, Ed. 2016.
40. USEPA PFAS Master List of PFAS Substances. https://comptox.epa.gov/dashboard/chemical_lists/pfasmaster.
41. Barzen-Hanson, K. A.; Field, J. A., Discovery and implications of C2 and C3 perfluoroalkyl sulfonates in aqueous film-forming foams and groundwater. *Environmental Science & Technology Letters* **2015,** *2* (4), 95-99.
42. Field, J.; Sedlak, D.; Alvarez-Cohen, L. *Characterization of the Fate and Biotransformation of Fluorochemicals in AFFF-Contaminated Groundwater at Fire/Crash Testing Military Sites*; Oregon State University Corvallis United States: 2017.
43. Kang, Q.; Gao, F.; Zhang, X.; Wang, L.; Liu, J.; Fu, M.; Zhang, S.; Wan, Y.; Shen, H.; Hu, J., Nontargeted

identification of per- and polyfluoroalkyl substances in human follicular fluid and their blood-follicle transfer. *Environment International* **2020,** *139*, 105686.
44. Washington, J. W.; Rosal, C. G.; McCord, J. P.; Strynar, M. J.; Lindstrom, A. B.; Bergman, E. L.; Goodrow, S. M.; Tadesse, H. K.; Pilant, A. N.; Washington, B. J.; Davis, M. J.; Stuart, B. G.; Jenkins, T. M., Nontargeted mass-spectral detection of chloroperfluoropolyether carboxylates in New Jersey soils. *Science* **2020,** *368* (6495), 1103-1107.
45. Chen, H.; Munoz, G.; Duy, S. V.; Zhang, L.; Yao, Y.; Zhao, Z.; Yi, L.; Liu, M.; Sun, H.; Liu, J.; Sauvé, S., Occurrence and Distribution of Per- and Polyfluoroalkyl Substances in Tianjin, China: The Contribution of Emerging and Unknown Analogues. *Environmental Science & Technology* **2020,** *54* (22), 14254-14264.
46. Li, Y.; Yu, N.; Du, L.; Shi, W.; Yu, H.; Song, M.; Wei, S., Transplacental Transfer of Per- and Polyfluoroalkyl Substances Identified in Paired Maternal and Cord Sera Using Suspect and Nontarget Screening. *Environmental Science & Technology* **2020,** *54* (6), 3407-3416.
47. Allred, B. M.; Lang, J. R.; Barlaz, M. A.; Field, J. A., Orthogonal zirconium diol/C18 liquid chromatography-tandem mass spectrometry analysis of poly and perfluoroalkyl substances in landfill leachate. *J Chromatogr A* **2014,** *1359*, 202-11.
48. Backe, W. J.; Day, T. C.; Field, J. A., Zwitterionic, Cationic, and Anionic Fluorinated Chemicals in Aqueous Film Forming Foam Formulations and Groundwater from U.S. Military Bases by Nonaqueous Large-Volume Injection HPLC-MS/MS. *Environmental Science & Technology* **2013,** *47* (10), 5226-5234.
49. Barzen-Hanson, K. A.; Davis, S. E.; Kleber, M.; Field, J. A., Sorption of Fluorotelomer Sulfonates, Fluorotelomer Sulfonamido Betaines, and a Fluorotelomer Sulfonamido Amine in National Foam Aqueous Film-Forming Foam to Soil. *Environmental Science & Technology* **2017,** *51* (21), 12394-12404.
50. Liu, J.; Mejia Avendano, S., Microbial degradation of polyfluoroalkyl chemicals in the environment: a review. *Environ Int* **2013,** *61*, 98-114.
51. Schymanski, E. L.; Jeon, J.; Gulde, R.; Fenner, K.; Ruff, M.; Singer, H. P.; Hollender, J., Identifying Small Molecules via High Resolution Mass Spectrometry: Communicating Confidence. *Environmental Science & Technology* **2014,** *48* (4), 2097-2098.
52. Goodrow, S. M. R., Bruce; Lippincott, R. Lee; Post, Gloria B., Investigation of Levels of Perfluorinated Compounds in New Jersey Fish, Surface Water, and Sediment. NJDEP, Ed. Trenton, N.J. : New Jersey Department of Environmental Protection, Division of Science and Research: 2020.
53. Moody, C. A.; Field, J. A., Perfluorinated surfactants and the environmental implications of their use in fire-fighting foams. *Environmental Science & Technology* **2000,** *34* (18), 3864-3870.
54. Gillison, A. N.; Jones, D. T.; Susilo, F.-X.; Bignell, D. E., Vegetation indicates diversity of soil macroinvertebrates: a case study with termites along a land-use intensification gradient in lowland Sumatra. *Organisms Diversity & Evolution* **2003,** *3* (2), 111-126.
55. Goodrow, S. M.; Ruppel, B.; Lippincott, R. L.; Post, G. B.; Procopio, N. A., Investigation of levels of perfluoroalkyl substances in surface water, sediment and fish tissue in New Jersey, USA. *Science of The Total Environment* **2020,** *729*, 138839.
56. Shoemaker, J. A. D. T., Method 537.1: Determination of Selected Per- and Polyfluorinated Alkyl Substances in Drinking Water by Solid Phase Extraction and Liquid Chromatography/Tandem Mass Spectrometry (LC/MS/MS). . U.S. Environmental Protection Agency, O. o. R. a. D., National Center for Environmental Assessment, Washington, DC, Ed. 2018.
57. Takarina, N.; Tjiong, G. P., Bioconcentration Factor (BCF) and Translocation Factor (TF) of Heavy Metals in Mangrove Trees of Blanakan Fish Farm. *Makara Journal of Science* **2017,** *21*.
58. Chen, C.-H.; Yang, S.-H.; Liu, Y.; Jamieson, P.; Shan, L.; Chu, K.-H., Accumulation and phytotoxicity of perfluorooctanoic acid and 2,3,3,3-tetrafluoro-2-(heptafluoropropoxy)propanoate in Arabidopsis thaliana and Nicotiana benthamiana. *Environmental Pollution* **2020,** *259*, 113817.
59. Li, Y.; Oliver, D. P.; Kookana, R. S., A critical analysis of published data to discern the role of soil and sediment properties in determining sorption of per and polyfluoroalkyl substances (PFASs). *Science of The Total Environment* **2018,** *628-629*, 110-120.
60. Zhang, W.; Zhang, D.; Zagorevski, D. V.; Liang, Y., Exposure of Juncus effusus to seven perfluoroalkyl acids: Uptake, accumulation and phytotoxicity. *Chemosphere* **2019,** *233*, 300-308.
61. Higgins, C. P.; Luthy, R. G., Sorption of Perfluorinated Surfactants on Sediments. *Environmental Science & Technology* **2006,** *40* (23), 7251-7256.
62. Uehara, G.; Gillman, G. P., Charge Characteristics of Soils with Variable and Permanent Charge Minerals: I. Theory. *Soil Science Society of America Journal* **1980,** *44* (2), 250-252.
63. Wang, N.; Szostek, B.; Buck, R. C.; Folsom, P. W.; Sulecki, L. M.; Gannon, J. T., 8-2 Fluorotelomer alcohol aerobic soil biodegradation: Pathways, metabolites, and metabolite yields. *Chemosphere* **2009,** *75* (8), 1089-1096.

64. Zhang, Y.; Meng, X.; Chai, T., Characterization of phenol-degrading Rhodococcus sp. strain P1 from coking wastewater. *Wei Sheng wu xue bao= Acta Microbiologica Sinica* **2013,** *53* (10), 1117-1124.
65. Amor, L.; Kennes, C.; Veiga, M. C., Kinetics of inhibition in the biodegradation of monoaromatic hydrocarbons in presence of heavy metals. *Bioresource Technology* **2001,** *78* (2), 181-185.
66. Moreira, I. S.; Amorim, C. L.; Carvalho, M. F.; Ferreira, A. C.; Afonso, C. M.; Castro, P. M., Effect of the metals iron, copper and silver on fluorobenzene biodegradation by Labrys portucalensis. *Biodegradation* **2013,** *24* (2), 245-255.
67. Levakov, I.; Han, J.; Ronen, Z.; Dahan, O., Inhibition of perchlorate biodegradation by ferric and ferrous iron. *Journal of Hazardous Materials* **2021,** *410*, 124555.
68. Tejirian, A.; Xu, F., Inhibition of Cellulase-Catalyzed Lignocellulosic Hydrolysis by Iron and Oxidative Metal Ions and Complexes. *Applied and Environmental Microbiology* **2010,** *76* (23), 7673-7682.
69. Joerss, H.; Menger, F.; Tang, J.; Ebinghaus, R.; Ahrens, L., Beyond the tip of the iceberg: suspect screening reveals point source-specific patterns of emerging and novel per-and polyfluoroalkyl substances in German and Chinese rivers. *Environmental Science & Technology* **2022,** *56* (9), 5456-5465.
70. Manz, K. E.; Feerick, A.; Braun, J. M.; Feng, Y.-L.; Hall, A.; Koelmel, J.; Manzano, C.; Newton, S. R.; Pennell, K. D.; Place, B. J.; Godri Pollitt, K. J.; Prasse, C.; Young, J. A., Non-targeted analysis (NTA) and suspect screening analysis (SSA): a review of examining the chemical exposome. *Journal of Exposure Science & Environmental Epidemiology* **2023**.
71. McCord, J. P.; Strynar, M. J.; Washington, J. W.; Bergman, E. L.; Goodrow, S. M., Emerging Chlorinated Polyfluorinated Polyether Compounds Impacting the Waters of Southwestern New Jersey Identified by Use of Nontargeted Analysis. *Environmental Science & Technology Letters* **2020,** *7* (12), 903-908.
72. Jacob, P.; Barzen-Hanson, K. A.; Helbling, D. E., Target and Nontarget Analysis of Per- and Polyfluoralkyl Substances in Wastewater from Electronics Fabrication Facilities. *Environmental Science & Technology* **2021,** *55* (4), 2346-2356.
73. Pieke, E. N.; Granby, K.; Trier, X.; Smedsgaard, J., A framework to estimate concentrations of potentially unknown substances by semi-quantification in liquid chromatography electrospray ionization mass spectrometry. *Analytica Chimica Acta* **2017,** *975*, 30-41.
74. Kruve, A., Strategies for Drawing Quantitative Conclusions from Nontargeted Liquid Chromatography–High-Resolution Mass Spectrometry Analysis. *Analytical Chemistry* **2020,** *92* (7), 4691-4699.
75. Nickerson, A.; Maizel, A. C.; Kulkarni, P. R.; Adamson, D. T.; Kornuc, J. J.; Higgins, C. P., Enhanced Extraction of AFFF-Associated PFASs from Source Zone Soils. *Environmental Science & Technology* **2020,** *54* (8), 4952-4962.
76. Banerjee, K.; Utture, S.; Dasgupta, S.; Kandaswamy, C.; Pradhan, S.; Kulkarni, S.; Adsule, P., Multiresidue determination of 375 organic contaminants including pesticides, polychlorinated biphenyls and polyaromatic hydrocarbons in fruits and vegetables by gas chromatography–triple quadrupole mass spectrometry with introduction of semi-quantification approach. *Journal of Chromatography A* **2012,** *1270*, 283-295.
77. Bu, Q.; Wang, D.; Liu, X.; Wang, Z., A high throughout semi-quantification method for screening organic contaminants in river sediments. *Journal of Environmental Management* **2014,** *143*, 135-139.

Appendices

(including the SOP for PFAS analysis by Nano-ESI-HRMS and a list of publications and presentations resulting from this project)

SOP for PFAS analysis by Nano-ESI-HRMS

Sample Preparation

Liquid and solid samples were extracted following protocols modified from EPA Methods 537 or 1633[9-10]. Then, extracts were filtered by 0.22-μm PES membrane and diluted in LC/MS-grade methanol. After spiked with the addition of 10 μL of the mixed internal standard (IS) solution, methanol-diluted samples were vigorously mixed and stored at 4 °C before the quantitative analysis and suspect screening by Nano-ESI-HRMS.

Nano-ESI-HRMS

Analysis of PFASs in the collected samples was conducted employing a high-resolution Q Exactive hybrid quadrupole−Orbitrap mass spectrometer (HRMS, Thermo Fisher Scientific, San Jose, CA) equipped with a Nano-ESI injector. The emitter tip was pulled using a laser puller (Model P-2000, Sutter Internet, Novato, CA). The capillary temperature was maintained at 350 °C throughout the analysis, which has been found to be most conducive for the ESI process. A pump was utilized to ensure a stable and consistent injection flow for the introduction of samples at 0.8 μL/min flow rate. An externally calibrated voltage regulator was coupled to the Nano- capillary emitter, which maintained at a negative charged voltage of -3.0 kV, to create ionization conditions. Furthermore, the automatic gain control (AGC) was set to achieve at least 100% target value (where the target value is defined to have a default intensity of 1e6), together with the total ion current (TIC) variation maintained below a 12% threshold until scan is done to ensure optimal signal stability and quality of spectral data acquisition across multiple scans. The resolution of 140,000 was selected for the HRMS with the spectra obtained based on a scan time of 2.0 min (80 scans). This ensures precision in the exact mass measurement and reliability of compound identification, in tandem with data-dependent acquisition (DDA) at a resolution of 80,000. For anionic PFASs, the operative mechanism of the HRMS instrument was set in the negative electrospray ionization (ESI-) mode.

The mass spectrometry first-level data (MS^1) was compiled by applying the full scan mode within the mass-to-charge ratio (m/z) range between 75 to 1,100 to obtain accurate comprehensive spectrum for target and non-target PFAS analysis, while the collision energy (CE) for this phase was set at a neutral 0. The data collection process encompassed 75 scans with each scan amassing an average data set from 5 micro-scans, resulting in an approximate detection time of 3.5 minutes.

Based on the suspect screening result of MS^1 data, potential m/z species were manually selected for collision-induced dissociation (CID) to collect MS^2 data. For select mass species of interest, MS^2 data were collected under the data-dependent acquisition (DDA) mode when CID was manually applied. The quadrupole filter was adjusted to differentiate the mass variance within ±0.2 Da, with a full-width half-maximum (FWHM) resolution of 500 (=m/dm) to provide identification of parent ions and their correlating daughter ions based on their co-occurrence in the second level of the mass spectrometry (MS^2) spectrum and the shifting relative intensity pattern reacted to the applied CE.

Upon the acquisition of the spectral data (MS^1 and MS^2), subsequent data analysis process was conducted to identify/quantify PFASs. A detailed integration of information would be conducted using the exact mass, stable isotopes, fragmentation, and fragment data from the DDA mode, as well as relative intensity data in both MS^1 and MS^2. The process would facilitate the determination of the chemical formula, confirmation of the structure of PFASs, and quantification of their concentration within a promising degree of confidence. This primary set of features was exported using the Xcalibur software (ThermoFisher Scientific, USA) as raw HRMS data files for further processing.

Custom-developed Python codes and R scripts were employed to: 1) interface with a local PFASs database, thus enabling the prediction of chemical formulas for selected peaks, 2) forecast the potential chemical structure of selected peaks using MS^2 data, and 3) identify of both apparent and significantly increasing peaks, a process achieved by conducting comparisons between respective experimental groups and their matching control groups.

Suspect Screening and Analyte Identification

Following Barzen-Hanson's work[27], the suspect screening method was developed to process Nano-ESI-HRMS data, consisting of four steps: local database construction, background noise removal, positive hit screening, and molecular structure validation.

A local PFAS database, consisting of the chemical formulae, SMILES structures, monoisotopic molecular weights, and putative monoisotopic anionic weight of ~7,300 PFASs, was constructed based on the Master List of PFAS Substances[40], "PubChem PFAS Tree", and timely updates from recent publications [8, 13, 21, 27, 41-50]. The Master List of PFAS Substances[40] (https://comptox.epa.gov/dashboard/chemical-lists/pfasmaster), maintained by EPA, is a comprehensive repository of PFAS. The PubChem PFAS Tree, (https://pubchem.ncbi.nlm.nih.gov/classification/#hid=120), on the other hand, serves as a navigable classification tree that would facilitate the exploration of PFAS and other fluorinated compounds within the PubChem database. Our assembled local database encapsulates a wealth of information for each PFAS compound, including the chemical formula, DTX-SID, preferred names, SMILES structures, average molecular weights, monoisotopic molecular weights, and putative monoisotopic anionic weights (cationic weights), data source and other pertinent information. To ensure the database remains current and comprehensive, it is routinely updated with newly identified PFASs, derived from recent scientific publications from journals and updates from EPA.

Background noise elimination is achieved by distinguishing mass species (m/z) unique in samples as compared to blanks and controls. Nano-ESI-HRMS analysis will produce a collection of mass species (m/z) and their associated relative intensities, termed as MS^1 data, which was extracted from the raw HRMS data file using Xcalibur software (ThermoFisher Scientific, USA). In order to distinguish analyte signals from background noise, a comparative analysis was performed between the peak lists of the samples and blanks. An array of blanks and controls were applied to monitor potential contamination and carryover, including instrument blanks (processed through same instrumental steps without known target PFASs), method blanks (PFAS-free solvent [i.e., methanol and acetonitrile] that were processed in the same manner as the sample extracts), site-specific reagent blanks (SSRBs, prepared with reagent water and transported to the sampling location, where the filled bottle's contents were subsequently exposed as the collected samples), lab-controlled reagent blanks (LCRBs, reagent water, methanol and acetonitrile in HDPE bottles, produced under laboratory circumstances). The designed criteria for background noise elimination

were established based on the relative intensity of the peaks from samples and controls. Specifically, any peak detected in the blanks or controls with a relative intensity surpassing 1,000 or exceed 0.01 of the corresponding peak's intensity in sample extracts was considered significant and thus subtracted from the MS^1 list to ensure the elimination of insignificant peaks for subsequent analysis.

The third step was to screen positive hits. The mass spectra, post background noise subtraction, were matched with the entries in our local database based on a mass error threshold of 5 ppm. Additional criteria were also employed for the screening of the positive hits, encompassing parameters, such as the absolute peak intensity and the relative intensity normalized to the internal standard (IS). Specifically, any positive hit exhibiting a relative intensity compared to the IS lower than 0.1% and any peak with an absolute intensity lower than 1,000 might not be further considered. A signal with such low intensity may not be reliable or sufficient for obtaining MS^2 data for further analysis. Following such screening criteria, the remaining peaks were collated into a suspect screening list and subsequently ranked based on their intensity.

During the validation phase, the structures of ions identified as positive hits were scrutinized using the fragmentation patterns derived from MS^2 data, obtained by CID. The confidence levels associated with the structure of suspect PFASs were subsequently determined based on a comprehensive evaluation of various data sources. These included MS data, MS^2 data, experimental data, library MS^2 data, and reference standards, in accordance with proposed guidelines by Schymanski et al. [51]. This validation process ensured that only reliable positive hits were considered for further analysis to provide accuracy identification of those peaks.

Python scripts (https://github.com/Daitoueqaq/HRMS-modification) were designed to execute several critical functions integral to the analysis of the suspect screening results. They can facilitate the extraction of chromatographic peaks from MS^1 data, perform noise deduction, align the experimental m/z of the suspects with the theoretical mass of PFAS in our database, and predict the likelihood of each peak in the MS^2 data. In addition, the scripts calculated the Kendrick mass defects and identified homologous series within the dataset. These functionalities collectively streamlined the suspect screening process and enhanced the accuracy of the analysis.

Absolute Quantification

A primary dilution standard (PDS) solution was prepared for the calibration of 22 target analytes (Table 1) via the dilution of the stock standard solutions in methanol (with 4% DI water) to achieve a concentration of 200 µg/L for each analyte. This PDS solution was serially diluted to prepare ten-point calibration solutions with 39 to 20,000 ng/L concentrations. All calibration solutions were prepared in triplicates, and their average mass intensities were used for constructing the calibration curves when the regression linearity met $R^2 > 0.99$. To assess the analytical sensitivity, the lower limits of detection (LODs) were determined for 22 target PFASs using the formula $3*S_B/m$, where S_B is the standard deviation of the target observed in blank controls and m is the slope of the calibration curve[38-39]. In case that a LOD is above the lowest calibration concentration (i.e., 39 ng/L), it is recalculated with the corrected slope after removing the lowest calibration point until the new LOD is below the lowest concentration used in the calibration.

Semi-Quantification

When the availability of commercial standards restricts absolute quantification for the analyte of interest (AOI), semi-quantification (SQ) can be an alternative. To estimate the concentration of the suspect PFASs in sample extracts, a streamlined SQ approach was developed

following previous reports[47-48, 72]. After structural examination by CID, PFAS AOIs were divided into five groups following a two-level classification scheme as depicted in Figure S1. In Level 1 classification, each PFAS AOI was primarily assigned into one of the three major groups based on its terminal functional group, including the sulfonate group -SO_3^-, the carboxylate group -COO^-, and the amide group -$CONH_2$, since terminal groups govern the ionization efficiencies in ESI. Level 2 classification is further based on the presence of alkyl carbons, particularly those adjacent to the terminal functional groups, as they interfere with the polarity distinctively from a perfluorinated chain. Four isotopic labeled ISs were assigned as the quantify marker (QM) for each group. Accordingly, appropriate calibration curves were used for semi-quantification by choosing the standards with similar functional moieties and chain lengths.

In SQ, an unknown analyte can be quantified by a different known analyte (quantification marker, QM) that shares similar chemical structure and ionization efficiency, albeit with uncertainty[73-75]. The choice of QM for the individual unknown analyte is critical for improving the estimation accuracy [20, 73]. The higher the structural similarity between AOI and its QM, the lower the quantification error derived from SQ[76-77]. Functional groups and molecular polarity are two major factors that affect ionization efficiency under ESI. In detail, group Sulfonates refers to the structures containing at least one sulfonate group (-SO_3^-). According to the polarity, group Sulfonates is divided into two sub-groups, PFSg, and FTSg. The former sub-group (PFSg) consists of the structures without non-fluorinated carbons, including PFSAs, cyclic-PFSAs, and chlorinated perfluorosulfonates (Cl-PFSAs). The latter sub-group (FTSg) consists of the structures with at least one carbon that is not fluorinated, such as the class of fluorotelomer sulfonates (FTSs), FTSASs, and FTSAS-SOs. Group Carboxylates refers to structures that have at least one carboxylate group (-COO^-) as the terminal group and is divided to two sub-groups, PFCg and FTCg. Similar to the group Sulfonates, PFCg refers to structures that don't contain non-fluorinated carbons, including the class of PFCAs, H-PFCAs, and O-PFCAs. Similarly, FTCg refers to the structures in which at least one carbon atom is not bound with fluorine, including the class of FTCAs, FTABs, and PFASACs[27]. The group Fluorinated Amides (FTAmg) refers to the structures containing the amide group (-(C=O)-NH-) as the terminal moiety. Specifically, the QM for the amide group was M2-6:2 FTCA due to the akin deprotonation behavior between the amide and carboxylic acid under the negative ESI mode.

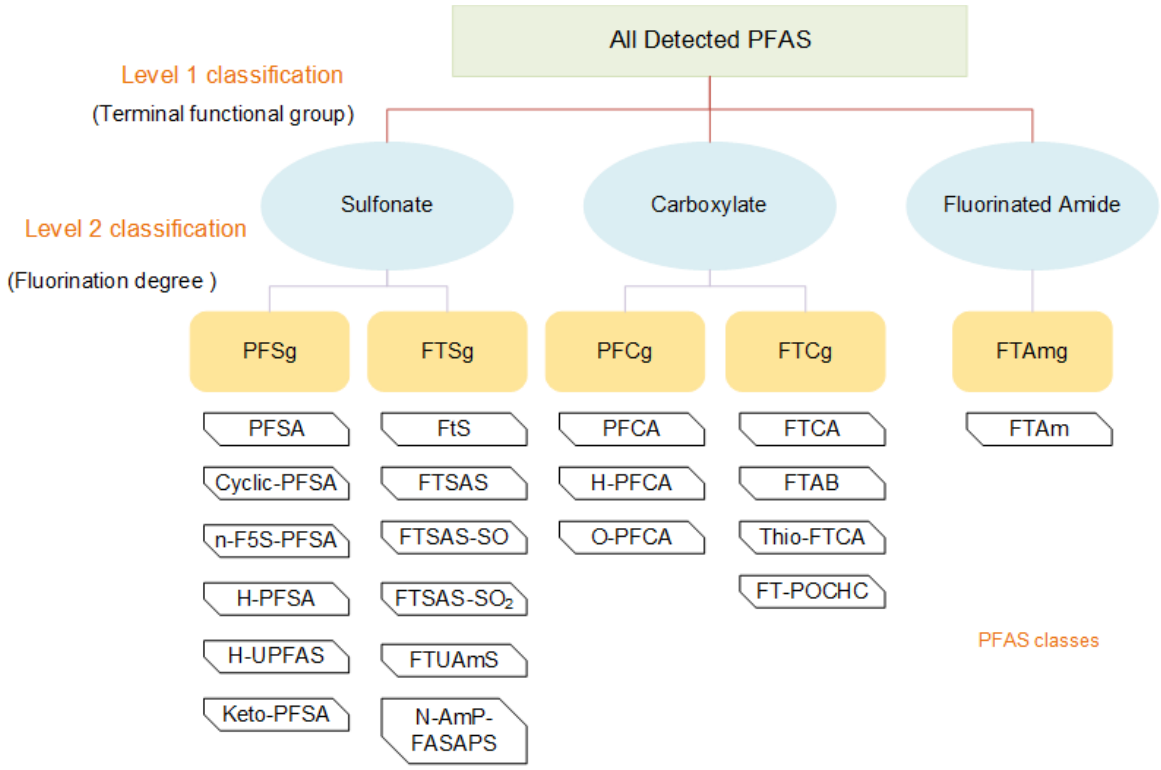

Figure S1. Grouping of the target and suspect PFASs for semi-quantification.

Publications

(1) Wu, C., S. Goodrow, H. Chen, and ***M. Li**** (2024). "Distinctive biotransformation and biodefluorination of 6:2 versus 5:3 fluorotelomer carboxylic acids by municipal activated sludge." Water Research 245, 121431. (DOI: 10.1016/j.watres.2024.121431)

(2) Su, B., S. Goodrow, H. Chen, and M. Li* (2023). "Conjugated biodefluorination products of FTCA biotransformation by *Rhodococcus jostii* RHA1." *(in preparation)*

(3) Wu, C., S. Yaqoob, S. Goodrow, and M. Li* (2023). "Impacts of substrates and heavy metals on FTCA biotransformation by *Rhodococcus jostii* RHA1." *(in preparation)*

(4) Wang, B., Rodriguez-Freire, L (2024) Poly-and perfluoroalkyl substances (PFAS) in water, sediment, soil and plants in potential contaminated areas in New Jersey (*in preparation*)

Conference Presentations

(1) Wu, C.*, Q. Wang, H. Chen, and ***M. Li***. (May 23, 2022) Target and Suspect Screening of Per- and Polyfluorinated Alkyl Substances (PFASs) in Municipal Wastewater Samples by Nano-ESI-HRMS. 2022 Chlorinated Conference. Palm Springs, CA. *(Poster)*

(2) Wu, C.*, Q. Wang, H. Chen, and ***M. Li***. (May 23, 2022) Aerobic Biotransformation and Biodefluorination of Fluorotelomer Carboxylic Acids (FTCAs) in Municipal Wastewater Treatment Sludge. 2022 Chlorinated Conference. Palm Springs, CA. *(Talk)*

(3) **Rodriguez-Freire, L.**, Wang, B., Dewson, S (June 2023) PFAS distribution in contaminated soils and impact on rhizosphere and plant microbiota, Environmental Chemistry meeting, Royal Society of Chemistry, University of Glasgow, UK.

(4) **Rodriguez-Freire, L.,** Wang, B., Dewson, S (September 2024) Catching PFAS: Engineering the plant microbiome for PFAS remediation. ISPTS meeting, Crete.